國立交通大學

機械工程學系

碩士論文

養豬場環境溫度對30kW沼氣渦輪發電機發電影響之實驗研究

The Experimental Study for Ambient Temperature Effect on 30 kW Turbine Generator Using Biogas in a Swine Farm

研 究 生：羅晨愷

指導教授：陳俊勳 教授

中華民國一〇三年六月

養豬場環境溫度對30kW沼氣渦輪發電機發電影響之實驗研究

The Experimental Study for Ambient Temperature Effect on 30 kW Turbine Generator Using Biogas in a Swine Farm

研究生　：羅晨愷　　Student：Chen-Kai Luo

指導教授：陳俊勳　　Advisor：Chiun-Hsun Chen

國 立 交 通 大 學

機 械 工 程 學 系

碩 士 論 文

A Thesis

Submitted to Department of Mechanical Engineering

College of Engineering

National Chiao Tung University

In Partial Fulfillment of the Requirements

For the Degree of

Master of Science

In Mechanical Engineering

June 2014

Hsinchu, Taiwan, Republic of China

中 華 民 國 一〇三年 六月

養豬場環境溫度對 30kW 沼氣渦輪發電機發電影響之實驗研究

學　　生：羅晨愷　　指導教授：陳俊勳

國立交通大學機械工程學系

摘要

本論文在台中月眉台糖養豬場測試 30 kW 沼氣微型渦輪發電機，使用處理後之不同濃度甲烷濃度之沼氣進行實驗，分析不同環境溫度和功率負載對發電機的性能影響。研究計畫第一部分，使用實驗數據並且利用 Brayton cycle 與組件之實際效率計算發電機之性能。結果顯示發電機之發電功率為 31.54 kW、熱效率為 25.62 %。第二部分在不同環境溫度下，測試不同負載(15~30 kW)之發電機效能變化，利用量測的數據分析發電功率和熱效率。結果顯示當環境溫度從 21.8 ^{o}C 上升至 31.4^{o}C，發電功率和熱效率分別下降 9.6%和 2.9%，且在發電機未到達引擎最大轉速額定功率 24 kW 下，甲烷質量流率從 0.1284 增加至 0.152 kg/min，顯示沼氣濃度不影響發電功率。第三部分，與國外研究之實驗數據作比較，探討不同燃料對 CR30 之性能影響。結果顯示發電機使用沼氣之淨輸出功率高於丙烷，但是使用沼氣之熱效率會

低於丙烷。淨輸出功率和熱效率之最大差異分別為 1.02kW 和 3.8%。最後，估計渦輪發電機沼氣發電之經濟效益，在 5,000 頭和 20,000 豬隻規模豬場使用渦輪發電機每年之發電量分別為 165,200 kWh 和 826,000 kWh、減碳量分別為 725 噸和 3,600 噸。

關鍵字:沼氣發電、渦輪發電機、環境溫度、經濟效益

The Experimental Study for Ambient Temperature Effect on 30 kW Turbine Generator Using Biogas in a Swine Farm

Student : Chen-Kai Luo　　Advisor : Prof. Chiun-Hsun Chen

Department of Mechanical Engineering

National Chiao Tung University

ABSTRACT

This research carried out the 30 kW micro-gas turbine engine (CR30) experiments using biogas in a swine farm in Taichung. The experiment used different concentrations of methane in desulfurized biogas to investigate the ambient temperature and workload effects on MGT. Firstly, the theoretical calculations were analyzed by use of Brayton cycle assumption with actual component efficiencies and experimental data as inputs. The results showed that the calculated generator power output and calculated thermal efficiency are 31.54kW and 25.62%, respectively. Secondly, under various workloads (15~30kW), the ambient temperature effects on performance of MGT are investigated. When the ambient temperature increases from 21.8 ^{o}C to 31.4 ^{o}C, the net power output and thermal efficiency decrease 9.6% and 2.9%, respectively. Besides, when MGT does not reach the maximum engine speed (~96,000 rpm), the methane mass flow rate increases from 0.128 to 0.152 kg/min at 24 kW of rated power output, indicating that CH_4 concentration in biogas does not affect the net power output. Thirdly, the comparisons with other researches were made for analyzing the effect by different fuels using CR30. By using biogas, it was found that the net power outputs are larger but the thermal efficiencies are lower than those by using propane. The maximum discrepancies of net power output and thermal efficiency are 1.02 kW and 3.8%, respectively. Finally, the economic benefits of MGT are estimated. The 5,000-pig and 20,000-pig swine farms can generate 165,200 kWh and 826,000 kWh of electricity per year and decrease 725 tons and 3,600 tons of CO_2 per year, respectively.

Keywords: Biogas Generation, Gas Turbine Engine, Ambient Temperature, Economic Benefits

ACKNOWLEDGEMENTS

首先感謝指導教授 陳俊勳教授，除了論文上的指導以外也教導我們未來職場上應有的工作態度及做人處事的道理。感謝宗翰學長在沼氣發電實驗中在旁的協助與指導，使我的實驗能順利進行。感謝昶安學長與家維學長在研究上給予我的協助。並感謝國科會計畫的經費支持使實驗能順利完成。

感謝同窗兩年的亞樵及惟翔，一起從碩一打拚到碩二畢業，謝謝你們的陪伴，使研究生活更加有趣。感謝學弟妹建豪、昭聖、沈為、宗志及心偉，有你們的幫忙及陪伴，使研究室更加熱鬧。感謝畢業學長泰全在實驗上給予的建議。

最後感謝栽培我的父母，謝謝您們從小的栽培與養育，成就現在的我，謹以此文獻給我的雙親。

CONTENTS

LIST OF TABLES

LIST OF FIGURES

Nomenclature

η_{isen}	Isentropic thermal efficiency
$\eta_{th,cal}$	Calculated thermal efficiency
$\eta_{th,actual}$	Actual thermal efficiency
η_T	Turbine isentropic efficiency
η_{comb}	Combustion efficiency
η_{mech}	Mechanical efficiency
η_C	Compressor isentropic efficiency
η_{HE}	Heat exchanger effectiveness
$\eta_{generator}$	Generator efficiency
Q_{ideal}	Ideal heat input
$Q_{th,cal}$	Calculated heat input
$Q_{th,actual}$	Actual heat input
W_T	Turbine output work
W_C	Compressor input work
$W_{T,isen}$	Isentropic turbine work
$W_{C,isen}$	Isentropic compressor work
$W_{net,power}$	Net power output
$W_{generator}$	Generator power output

Nomenclature

$W_{consumption}$	Micro-gas turbine internal consumption
r_p	Pressure ratio
T_0	Measured ambient temperature
T_1	Measured compressor inlet temperature
T_{2s}	Isentropic compressor outlet temperature
T_2	Compressor outlet temperature
T_3	Heat exchanger outlet temperature (air side)
T_{3s}	Isentropic heat exchanger outlet temperature (air side)
T_4	Combustor outlet temperature
T_{4s}	Isentropic Combustor outlet temperature
T_5	Isentropic turbine outlet temperature
T_{5s}	Turbine outlet temperature
T_6	Heat exchanger outlet temperature (gas side)
T_{6s}	Isentropic heat exchanger outlet temperature (gas side)
T_{biogas}	Temperature of treated biogas
P_1	Compressor inlet pressure
P_2	Compressor outlet pressure
P_3	Combustor inlet pressure
P_4	Turbine inlet pressure
P_5	Turbine outlet pressure
P_6	Heat exchanger outlet pressure
$\Delta P_{recuperator}$	Pressure drop of recuperator
$\Delta P_{combustor}$	Pressure drop of combustor

Nomenclature

$C_{p,air}$	Air specific heat capacity at constant pressure
C_{p,CH_4}	Methane specific heat capacity at constant pressure
$C_{p,biogas}$	Biogas specific heat capacity at constant pressure
$C_{p,gas}$	Hot gas specific heat capacity at constant pressure
$\dot{m}_{air}$	Air mass flow rate
$\dot{m}_{biogas}$	Biogas mass flow rate
$\dot{m}_{CH_4}$	Methane mass flow rate
$\dot{m}_{gas}$	Hot gas mass flow rate
LHV	Lower heating value

Chapter 1

Introduction

1.1 Motivation and Background

Nowadays the global warming has become worse and worse due to the increasing concentration of greenhouse gases, which include carbon dioxide, chlorofluorocarbons, nitrous oxide, water vapor, methane etc., in atmosphere. The major contributor is carbon dioxide resultant from the combustion of fossil fuels, which plays the main role of power supply to mankind after industrial revolution. Figure 1.1 [22] shows the global carbon dioxide emission that especially grows so quickly from 1965 to 2013. In addition, with the increase of energy demand, the fossil fuels are expected to deplete in upcoming decades. Therefore, the researches of alternative energy are developed and their scales are expanded to respond to Green House effect and energy crisis.

In Taiwan, the main energy resources are from petroleum and coal that occupy 80% of total energy consumption per year. The percentage for the individual energy resource used in Taiwan's power supply is shown in Fig. 1.2 [23]. It shows that only a small proportion of power consumption was from renewable energy in 2013, indicating that the development of related fields was insufficient. Furthermore, the imported energy resource reached 88.2% of the entire power supply in 1988, 99.3% in 1998 and 99.3% in 2013, showing that the energy resources depends on other countries significantly and they mainly are fossil fuels. As mentioned previously, these energy resources will produce a large amount of GHG, especially through thermal power generation. It is very crucial to decrease the dependence of imported energy for the reason national security. Hence Taiwan's energy policy devotes to develop other energy sources, such as nuclear power and renewable energies, for the sustainability of industry sector and the low-carbon society.

However, the Lungmen nuclear power plant in Taiwan is a controversial issue, especially as the Fukushima nuclear power plants were almost destructive completely on March 11, 2011 by a severe earthquake occurred in the Western Pacific Ocean of Japan. The tsunami destroyed the cooling system of power plant and led to the meltdown of atomic reactors. The radiation pollution greatly affected the Japanese health and their related industry. For this reason, many Taiwanese show their intense concern on the Lungmen nuclear power plant and hope to stop building it.

In order to resolve the shortages of energy (including the stop running of nuclear power plants) and reduce carbon dioxide emission, the development of renewable energy in recent years has attracted many researchers' attention. They include wind, solar, water and bio energy. This research is focus on power generation from gas turbine by using biogas, which is a kind of bioenergy. Bioenergy becomes more and more popular due to its advantage of stable supply and the contribution to environmental protection. Figure 1.3 shows the potential of biogas in Taiwan, which comes from different sources, including livestock waste, family waste water, landfill, industrial waste water. It can be found that the livestock waste is a main source of biogases and its quantity about $6\times 10^8\ m^3$ per year.

In Taiwan, the main livestock is swine and their manure is a big impact on the environment. Thus, this study engages in using manure to produce biogas to generate the electric power and simultaneously alleviate the pressure of manure on environmental protection issue. Figure 1.4 shows a simple carbon cycle for biogas. Plants catch carbon dioxide from the atmosphere by photosynthesis, which uses solar radiation. Then, the livestock eat plants and discharge manure, which pollutes the environment. The pollutions can be treated by wastewater treatment system for alleviating the impact on environment and producing the biogas. The piston or gas turbine engine/generator can utilize biogas via combustion to produce electricity. Finally, the engine discharges the carbon dioxide to atmosphere. Thus, biogas can be regarded as a carbon neutral energy resource since it is produced from waste. This study uses biogas to supply a 30-kW gas turbine to generate electricity in a swine farm that is a continuous effort of Ge's study [4]. The biogas is flammable because its contents mostly consists of methane (CH_4), and the others are carbon dioxide (CO_2), ammonia (NH_3), hydrogen (H_2), nitrogen (N_2), hydrogen sulfide (H_2S), and a small amount of organic compounds. In Ge's study [4], the economic benefits of using biogas with 5,000 pigs were estimated. The results showed that it can totally generate 219,000 kW-h of electricity from the biogas and the corresponding CO_2 can be decreased by 5000 ton/year. Apparently, CO_2 emission and usage of fossil fuel can be reduced by using biogas in turbines.

This laboratory has been awarded a four-year research project by National Science and Technology Program for Energy from 2010 to 2013. The project is named as *Development of the technology of agricultural* *waste bioconversion to biogas for electricity generation and Carbon dioxide elimination by microalgae*. Constructing a pilot biogas power plant is the ultimate goal of this project, which divided into four subprojects. The subproject 1 is to upgrade the utilization efficiency of biogas by removing hydrogen sulfide (H_2S) and CO_2 to improve the biogas generation rate. The concentration of H_2S is 5000 ppm in untreated biogas, stored in anaerobic tank. The high concentration H_2S will corrode the turbine engine, so the H_2S biological desulfurization system, developed by the subproject 1, was installed such that it could reduce H_2S concentration from 5000 to 50 ppm effectively. In the subproject 2 (present research), the desulfurized biogas of subproject 1 is utilized to operate the engine to produce electricity under different monitoring parameters. The subject 3 is to produce biodiesel from high lipid-content algae utilizing waste CO_2 either from the engine flue gas or the biogas itself. The purpose of the subject 4 is to investigate the operating conditions that affect biogas production rates and methane concentration emission during the anaerobic processes.

This study is subproject 2 that produces electricity by using turbine engine. In the first year of the project, Lin [1] used a 30 kW piston engine to construct a waste heat recovery system and to analyze the power output and thermal efficiency under different excess air ratios. Furthermore, the effect of oxygen-enriched combustion for engine was also tested. In the second year, Huang [2] applied a waste heat recovery system to analyze the preheating influence on the performance of power generation. Followed by Wu [3], a complete ignition measurement system was installed, consisting of spark plug pressure sensors and rotary encoder, to record the in-cylinder pressure and crank angle of piston cylinder. He found the optimum spark timing provides the highest power production, thermal efficiency and CH_4 utilization.

In 2013, Ge [4] tested the gas turbine engine by using 67% methane content of biogas. The performance of turbine engine under various operating loads was tested, and the energy analysis for micro turbine engine was studied. Besides, the comparison of CH_4 consumption, thermal efficiency, air flow rate and biogas supply rate were analyzed by using piston and turbine engines. He found that the turbine engine speed will restrict the maximum power generation (25.23 kW), and the air flow is higher than the one in piston engine. In addition, under low workload, turbine engine can offer more stable power generation than piston engine. This study extends Ge's experiments with different operating conditions and considers an important parameter, the ambient temperature. Consequently, the detailed theoretical calculations of turbine engine performance are carried out to investigate the exit temperatures for each component by thermodynamic formula and a comprehensive comparison with the work of Vidal et al. [19] is given.

1.2 Literature Review

Lin [1] tested different air-fuel ratios for 30 kW generator with 60% methane concentration of biogas in a swine farm in Miaoli, Taiwan. The oxygen-enriched combustion and waste heat recovery were also applied to his research. The results showed that a higher power output and better thermal efficiency can be achieved by a greater conversion of CH_4 in the combustion process. The engine performances are not improved by 1% oxygen-enriched air. However, with 3% oxygen-enriched air, the maximum power generation and thermal efficiency increase, also the engine can operate at a lower limiting fuel supply rate. The waste heat recovery system is used to heat up water, which replaces the heating of nature gas and electricity, leading to an improvement of overall efficiency.

Huang [2] conducted experiments with 73% CH_4 concentration of biogas to compare with the results of Lin [1] and applied the waste heat recovery system to preheat the inlet biogas under different temperatures. Also, Huang analyzed the preheating influence on the generation performance. The results showed that the power generation with 73% CH_4 of biogas are higher than the one with 60% CH_4 of biogas, except in the region around $\lambda < 0.85$. However, the thermal efficiency increases with the increasing methane concentration in the region of $\lambda > 0.95$. In the case of the increasing inlet biogas temperature effect, there is an obvious improvement on thermal efficiency when the temperature increases from 40 to 120 ℃ with 140 L/min biogas supply rate and λ=1.58.

Wu [3], the same as Lin [1] and Huang [2], used the same type of biogas generator and operated it under similar conditions to study the effects of the water vapor content in biogas and the spark timing on generator. The results showed that within a certain range of biogas supply rate, the biogas with dehumidification provides higher power generation and thermal efficiency than the one without dehumidification. The power outputs increasing rates under the biogas supply rates of 200, 220 and 240L/min at stoichiometric condition are up to 4.7, 5.9 and 2.7%. The dehumidified biogas offers enthalpy increasing rate up to 0.79%, 1.17% and 1.27% better than the biogas without dehumidification. Besides, the optimum spark timing of present engine is located at BTDC13, which can supply larger power output than the other spark timings. At a given biogas supply rate and excess air ratio, the power generation, thermal efficiency and CH_4 utilization by operating at the spark timing of BTDC13 are the highest.

Ge [4] tested the 67% methane content of biogas by using gas turbine engine. The performance of turbine engine under various operating loads was tested, and the energy analysis for micro turbine engine was studied. Besides, the comparison of CH_4 consumption, thermal efficiency, air flow rate and biogas supply rate were analyzed by using piston and turbine engines. The economic benefits were also estimated by the data obtained with 3000 and 5000 pigs in this research. He found that the engine speed will restrict maximum power generation (25.23 kW), and the air flow rate of turbine engine is higher than piston engine. In low workload, turbine engine can offer more stable power generation than piston engine. The results also showed that the range of biogas flow rate for the turbine engine is from 184.9 to 251.8 L/min under varying loads ranged from 15 to 30 kW, and the maximum power generation, the corresponding thermal efficiency and the CH_4 consumption rate is 25.23 kW, 23.12% and 168.7 L/min, respectively. For piston engine, the maximum power generation, the corresponding thermal efficiency and the CH_4 consumption rate is 26.48 kW, 26.37% and 155.2 L/min, respectively. The estimated economic benefits showed that the net turbine power generation of 5000 pigs is greater than piston engine.

Cornelissen et al. [5] presented detailed analyses of the supply potential and the use of biomass in the context of a transition to a fully renewable global energy system by 2050. They also investigated bioenergy potential within a framework of technological choices and sustainability criteria, including the criteria on land use and food security, agricultural and processing inputs, complementary fellings, residues and waste. They found the potential for sustainable bioenergy from residues and waste, complementary fellings, energy crops and algae oil in 2050. The maximum of 2,500,000 km^2 cropland is needed and a 75%-85% reduction of greenhouse gas can be achieved compared to fossil references.

Tsai and Lin [6] surveyed bioenergy from livestock manure management in Taiwan. With the practical characteristics of the total swine from the farm scale of over 1000 pigs, the quantity of methane generation from livestock was calculated (Gg). The results showed the following benefits (about 4.3 million pigs): emissions of methane is reduced to 21.5 Gg/year, total generated electricity is 7.2×10^7 kWh per year, equivalent to electricity charge saving of US$ 7.2×10^6 and carbon dioxide mitigation of 500 Gg per year.

Su et al. [7] built a greenhouse gas production database from anaerobic livestock wastewater treatment processes in Taiwan, and made the comparison between the livestock wastewater treatment system presented by the IPCC with that used in Taiwan. Analysis of GHG samples from in situ anaerobic wastewater treatment systems of pig and dairy farms revealed, respectively, average emissions of 0.768 and 4.898/kgCH_4, 0.714 and 4.200/kgCO_2, and 0.002 and 0.011/kgN_2O per pig in one year during three temperature periods, whereas average temperatures is <20, 20–25, and >25◦C. Average emissions rates of CH_4 from selected pigs and dairy farms are lower than the limits imposed by the IPCC, because livestock manure is diluted before being treated with a solid/liquid separator and an anaerobic wastewater treatment system.

Basrawi et al. [8] investigated the effect of the inlet air temperature on the performance of micro gas turbine (MGT) with cogeneration system (CGS) arrangement. They used the model of the MGT-CGS to test the system performances by setting up on the basis of experimental results obtained in a previous study and a standard data that defines season interval. It was simulated under different ambient temperature conditions in a cold region. The results showed when temperature increases the electricity of the MGT decreases, but ratio of exhaust heat to mass flow rate and exhaust heat recovery to mass flow rate increases in summer peak. Furthermore, they also compared total energy efficiency, fuel energy saving and CO_2 with two conventional systems. Besides, the MGT annually reduces 30,000-80,000 m^3 of fuel consumption and 35-94 ton of CO_2 emissions.

Kang [9] investigated the effect of firing biogas on the performance and operating characteristics of gas turbine. The simple and recuperative cycle engine was simulated in a similar power output. They tested it with biogas under different methane concentrations and found that gas turbine efficiency increases with decreasing methane concentration in the simple cycle engine, but efficiency decreases in the recuperative cycle engine. The CH_4 content decreases with the decrease of net efficiency. Moreover, the heat recovery also increases by firing biogas. However, the reduction of the compress ratio and overheating of the turbine blade led to the increase of turbine flow. The results provide useful information for the operating strategies of biogas-fired gas turbine under the simultaneous limitations by the compressor surge and turbine overheating.

De Sa et al. [10] employed specific turbines SGT 94.2 and SGT94.3 in experiments installed at the DEWA Power Station which is located in Dubai, UAE. The purpose of the study was to obtain empirical relationship between the gas turbine's ability to generate power when exposed to site ambient conditions, such as the ambient temperature. They tested the gas turbine thermal efficiency and useful power output under various ambient temperatures in different workloads. The results showed that the high ambient temperature leads to low thermal efficiency and useful power output. The gas turbine loses 0.1% thermal efficiency and 1.47MW of its Gross Power Output with every increase by 1 Kelvin. The gas turbine inlet temperature being a limiting factor as dictated by the turbine blade metallurgy and mass flow of air being is reduced at high temperature.

Erdem et al. [11] considered two gas turbine models and seven climate regions in Turkey. For both models, by using average monthly temperature data of regions, both the annual electricity production loss and fuel consumption increase compared to those in standard design conditions. The result showed that the electricity production loss about 2.87-0.71% compared to standard production occur in hot regions. When the temperature is above standard ambient temperature by 15 degree Celsius, electricity production loss rates would vary between 1.67% and 7.22%. Therefore, when the inlet temperature decreases to 10 degree, electricity generation increases from 0.27 to 10.28%.

Strub et al. [12] simulated the system by changing inlet air temperature with phase change refrigeration storage. The selected turbine was a land turbo-alternator that burned oil or natural gas and were used for Combined Heat and Power generation. The results showed that the volume of storage tank affects the electric output. The 51.5 m^3 volume storage has enough electricity power to meet the New Delhi's requirement due to the phase change materials can absorb more heat.

Yamada et al. [13] investigated the suitable size (electricity output capacity) for micro gas turbine cogeneration systems (MGT-CGSs) depending on scale of the sewage treatment plant and the effect of ambient temperature on heat demand of the plant performance under three ambient temperature conditions. They used the optimal combination of MGT-CGSs with different sizes, 30kW, 65kW, 200kW, and tested in different scales of the sewage treatment plant. The results showed that ratio of heat demand to energy of biogas produced increases when scale of the sewage treatment plant decreases, and the MGT has approximately the same fuel energy input under full load as the biogas energy produced in the plant has the highest efficiency. Furthermore, MGT-Combination has the highest efficiency but its efficiency will be the same as that of the other MGT-CGSs when only comparatively constant operation is required throughout the year such as operation in a tropical region.

Wu [14] applied a commercial package CFD-ACE+ to simulate the combustion flow field in combustion chamber of a micro gas turbine. The research focused on the applications of CFD simulations on low heating value methane gas fuel for the acceptability of MV54 micro gas turbine. Two parameters were studied. One is the mass fraction of CH_4 in the fuel mixture, consisting of CH_4 and CO_2, and the other is the turbine rotational speed. The simulation results showed that the thrust diminishes again as a result of adding non-fuel substance (CO_2) into pure methane fuel. It also indicated that the total air mass flow rate of primary zone decreases with the reduction of turbine rotational speed. In addition, the flow field was analyzed by selecting the cross-sections, locating at symmetric face. The result showed that the CH_4 mass fractions and temperature in primary zone increase with rising methane level.

Basrawi et al. [15] simulated two micro engine systems, cogeneration system (CGS) and trigeneration system (TGS). The two systems are used in residential buildings located in the area with tropical climate. The energy, economic and environmental performance of MGT-CGS and MGT-TGS were studied. The MGT-CGS consists of an MGT and an exhaust heat exchanger (EHE), whereas MGT-TGS equipped with other equipments such as an absorption heat pump and a heat storage device. The results showed that the payback period for the MGT-TGS is 13.8 years shorter than MGT-CGS, 14.3 years. The

MGT-TGS also has a higher Fuel Energy Saving Index FESI when compared to a gas turbine, but had a lower FESI when compared to a combined cycle gas turbine.

Lee et al. [16] used microturbines to promise power sources for small scale combined heat and power (CHP) systems. The power output and efficiency of microturbine decrease when ambient temperature increases. They also set up an analysis program for simulating the operation of a microturbines CHP system. The injection of water or steam into a microturbines CHP system was analyzed. The injection of hot water, which is generated at the heat recovery unit, at two different locations inside the microturbine was predicted. The results showed that injection at the recuperator inlet gives a higher efficiency than injection at the combustor in both water and steam injections. Steam injection provides a higher power generation efficiency than water injection on the average. The injection of steam at the recuperator inlet is most promising in terms of power generation efficiency. However, water injection at the recuperator also enhances power generation efficiency while still provides thermal energy to some extent.

Sheng et al. [17] investigated the effect of the ambient temperature on the performance of gas turbine since the electricity production, fuel consumption and plant incomes are affected by temperature. They found that the power decreases due to reduction in air mass flow rate and the efficiency decreases because the compressor requires more power to compress air in high temperature.

Bakalis and Stamatis [18] used the hybrid system, consisting of solid oxide fuel cell and Capstone micro-gas turbine system. The system was simulated in Aspen Plus^{TM} process simulator and analyzed its exergy destruction, the amount of work obtainable when the system is in unbalance state. The results showed that the SOFC stack and burner have the higher destruction rate of exergy. There is a large amount of exergy loss because of exhaust gases. And if the SOFC stack temperature is enhanced, the system exergy efficiency will increase. Besides, the CO_2 emissions can be decreased by using this system mentioned above.

Vidal et al. [19] structured a simple model for the Capstone 30kW micro gas turbine and carried out the simulations at high ambient temperatures under the maximum rated power output to analyze the corresponding performance. Moreover, the turbine was working in a high-pressure system and a gas/water heat exchanger was installed to heat the cold water. This study adopted the experimental data, obtained from the CREVER research centre (Tarragona, Spain) by using propane to simulate the performance of MGT, as the initial conditions. The MGT model was simulated by Aspen Plus software (Aspen Plus, 2004), which can proceed the different steady state modeling applications. The results showed that the net output power decreases with increasing ambient temperature. The net power decreases 5.1% as the ambient temperature is raised from 24.4 to 28.9°C and the electrical efficiency has 2% reduction.

Leszek and Monika [20] analyzed the energy and exergy with sample device for micro turbines. The model applied the Brayton cycle and heuristic part-load performance formulas, and it was validated using the experimental data for a 30 kW micro gas turbine provided by Capstone. The results showed that the exergy destructions of the combustion chamber and recuperator are the main losses. The efficiency of the recuperator can be increased when the air temperature enhances. A higher air temperature causes a less exergy destruction at the inlet of the combustion chamber.

Homam Nikpey Somehsaraei et al. [21] investigated the fuel flexibility and performance of micro gas turbine (100 kW). In order to achieve this purpose, the thermodynamic model (IPSEpro) was adopted and simulated the results by using experimental data obtained from T100 MGT in Stavanger, Norway. They analyzed the influences of the fuel change by replacing natural gas to biogas in different conditions, such as ambient temperature and power output. The results showed that the electrical efficiency and recuperator effectiveness decrease with an increase of power output, however, these will decrease with ambient temperature. The contents of methane (45, 60, and 70%) in biogas change the properties of fuel, so the power output and electrical efficiency of biogas decrease with the decreasing percentage of methane in biogas. Because of this reason, the biogas fuel mass flow rate is larger than natural gas one.

1.3 Scope of Present Study

The scope of this research is presented in Fig. 1.5. First, the treated biogas stored in the tank will be sucked into the combustion chamber when turbine engine is working. The components of biogas are measured by Gas Analyzer (IR-208) before entered into the engine, which is Capstone CR30 Micro Turbine engine, provided by the Aerospace Industrial Development Corporation (AIDC). The workloads vary from 15 to 30 kW and air flow and biogas supply rate change with the load accordingly and automatically. The biogas and air flow rates are recorded for analyzing performance of turbine engine. Since the influences of ambient temperature on the performance of gas turbine engine is very important, hence the performance of gas turbine engine are tested under different ambient temperatures (15~35^{o}C) and loads (15~30 kW). The components of exhaust gases are also recorded. The gas turbine performance is analyzed by using thermodynamic formula to investigate the energy balance and entrance temperatures, which cannot be measured directly. Then, a comprehensive comparison with the work of Vidal et al. [19] is given to justify the effect of ambient temperature. Finally, the economic benefits are estimated by using C30 data, such as the electricity generation, equipment cost, maintenance cost et.al, to obtain the payback period and electricity cost per kWh and to estimate the potential application of biogas in Taiwan by using gas turbine engine.

Chapter 2

Biogas Generation System

2.1 Process of Biogas Production

The manure of swine is pretreated by using the three-step piggery wastewater treatment system to produce biogas, which has a hydrogen sulfide (H_2S) will corrupt the engine. Fig. 2.1 and Fig. 2.2 show the process of biogas production including solid/liquid separation, anaerobic treatment and aerobic treatment (activated sludge treatment system). The manure of swine is collected and treated with wastewater treatment system. First, the separation of the solid from the waste water is to reduce the content of solids for subsequent handling and treatment, and to recovered solids can be used as fertilizer, etc. This physical process is accomplished by using various kinds of filters. Secondly, the anaerobic treatment which is conducted after solid/liquid separation, and occurs inside of anaerobic basins enclosed with "red-mud plastic (RMP) cover" (1.2~1.8mm of thickness), made of a kind of PVC material, which is corrosion-resistant and gas-and-water impermeable. Besides, the anaerobic treatment system can salvage a part of chemical energy content of wastewater by producing methane.

The anaerobic tank contains very high content of hydrogen sulfide (H_2S), which can corrupt the power generator, so the desulfurization system is needed to remove H_2S. The common method for reduction of hydrogen sulfide is biological desulfurization. In the process, the H_2S is absorbed in water and then its content is reduced effectively by using biological method. Finally, the biogas will be stored in a red plastic bag after the desulfurization process.

2.2 Utilization of Biogas

From 1990, the animal husbandry has been blooming in Taiwan, so the pollution of manure become more serious. In order to solve this problem, the three-step piggery waste water was built, which can produce biogas. There are some usages of biogas, ex: domestic fuel of gas stove, water heater. Besides, the application of power generator by using biogas had paid attention and expanded the scale gradually. The combined heat and power (CHP) generation plants is popular used in a four-stroke or a Diesel engine. The CHP generation can produce heat and power for higher energy efficiency simultaneously. It is a general way to transform energy of biogas at small or large-scale plants of biogas production.

Fig. 2.3 shows the range of capacities for the power generators, which are available on the market for the pilot-plant or industrial scale. The efficiency is defined as the ratio of the electrical power generated to the total energy content in the biogas. Efficiency figures are also provided by different manufacturers. Small-capacity engines generally can result in the lower efficiencies than that of high-capacity engines.

The generated electricity and heat can supply to the bioreactor itself, associated buildings, and neighboring industrial companies or houses. The power can be fed into the public electricity network, and the heat into the network for long-distance heat supply.

2.3 Engines

Table 2.1 presents some engines that can be operated with biogas. These have been improved during the recent years by developing the works which are inspired by the worldwide boom in biogas plants. Some manufacturers have already had the engine performances better than presented the Table 2.1.

Table 2.1 Comparison of Different Power Generators

Feature	Four-stroke engine	Gas-Diesel engine	Stirling engine	Fuel cell	Gas turbine	Micro gas turbine
Capacity(kW)	<100	>150	<150	1-10000	20MW	28-200
Electrical efficiency	30-40%	35-40%	30-40%	40-70%	25-35%	15-25%
Pressure ratio	10:1	20:1	5:1	n.a.	5:1	5:1
Lifetime	Medium	Medium	Long	Very short	Long	Long
Alternative fuel in case of shortage of biogas	Liquid gas (gasoline)	Liquid gas	Any	Natural gas	Natural gas	Natural gas, Fuel oil

2.3.1 Micro Gas Turbine

Micro gas turbines are small high-speed gas turbines with low combustion chamber pressures and temperature, which are designed to generate the electrical powers between 28kW to 200kW. They are operated on a Brayton cycle, consisting of a gas compressor, a combustion chamber and an expansion turbine. This study use the CR30, which is micro gas turbine. For normal operation, the compressor sucks in the combustion air. The fuel is normally supplied to meet the combustion air in the combustion chamber. When biogas with a low calorific value is used, it must be adjusted to a flammable mixture of biogas and air before it is supplied into the combustion chamber.

The electrical efficiency of 15~25% for today's micro gas turbines is still unsatisfactorily low. An attempt to increase the efficiency has been made by preheating the combustion air in heat exchange with the hot turbine exhaust gases. But great improvements are still necessary before micro gas turbines can be introduced into the market of industrial biogas plants. However, the coupling of a micro gas turbine with a micro steam turbine to form a micro gas-steam turbine seems already interesting and economical today because of its high electrical efficiency.

2.3.2 Gas Turbine

Biogas can be converted to current via gas turbines of medium and large capacity (20 MW and more) at a maximum temperature 1200 ℃. The tendency is to go to even higher temperatures and pressures, whereby the electrical capacity and thus the efficiency can be increased. The main parts of a gas turbine are the compressor, combustion chamber, and turbine.

Ambient air is sucked and compressed in the compressor and transmitted to the combustion chamber, where biogas is introduced and burnt with the compressed air. The flue gas that is so formed is passed to a turbine, where it expands and transfers its energy to the turbine. The turbine propels the compressor on the one hand and the power generator on the other hand. The exhaust gas leaves the turbine at a temperature of approximately 400~600 ℃. The waste heat can be recovered by driving a steam turbine downstream for heating purposes or for preheating the air that is sucked into the combustor

Chapter 3

Experimental Apparatus and Procedures

3.1 Experimental Layout

The Experiment layout and biogas pretreatment system are shown in Figure 3.1. The flow meter measuring the biogas flow rates is installed in front of inlet of combustor. The flow meter is automatically adjusted according to the change of engine load. The biogas and air flow rates are shown in flow meter and sucked into the combustion chamber when the turbine engine starts. In order to prevent turbine blade from heat damage, most of air will be used to cool the hot gas which is from outlet of combustion chamber. The desulfurized biogas is moved to biogas storage for this experiment.

First, the biogas will pass through the cyclone and filter for removing the liquid water and impurities which damage the engine. Then, the front compressor which treats biogas will increase the pressure and temperature of biogas by reducing its volume for corresponding pressure of combustor. The compressor outlet temperature is about 40 ^{o}C, and the pressure of biogas is 5 kg_f / cm^2. Secondly, the biogas will pass through Freeze dryer to remove water vapor for enhancing power output [3], the biogas temperature is reduced to 36 ^{o}C. Finally, the biogas will be stored in the biogas tank whose capacity is 800 liters for maintaining the pressure (5.6 kg_f/cm^2), and then the biogas is mixed with air and ignited in the combustor. Besides, the compositions of waste gases are measured by gas analyzer (IR-208), which is set at the engine outlet, and the waste gas temperature is measured by K-type thermocouple.

The electricity produced by micro-gas turbine (MGT) will supply to biogas pretreatment system for reducing energy consumption (~ 0.7 kW) from other power sources. Those devices include freeze dryer and compressor. Finally, the electricity is recorded by the power meter and supplied to parallel electric grid.

3.1.1 Micro-Gas Turbine Engine (CR30)

Figure 3.2 shows the schematic procedure of micro-gas turbine engine. The main components include centrifugal compressor, radial turbine, annular combustor and annular recuperator. The compressor, turbine and generator are mounted on the same shaft which is supported by patented air bearings and can spin at up to 96,000 RPM. The turbine provides power to drive compressor and generator.

First, the air passes through the air filter to remove the impurities, and then absorbs the heat from cooling fin of generator to protect generator from heating damage. Afterward, the air will be accelerated and pressured by compressor for attaining the limitations of pressure in combustion chamber, and then the compressed air will pass through the recuperator to enhance its temperature for reducing the consumption of fuel and increasing thermal efficiency. The fluid of heat exchanger is exhaust gases which are exhausted from outlet of turbine engine. Next, the air will be mixed with treated biogas and sucked into combustor for igniting. Finally, the hot gases drive the blades of turbine to generate electricity.

CR30 is controlled by digital power controller (DPC), which mainly controls the fuel valve, engine speed and turbine outlet temperature. In order to control the net power output, the DPC commands the fuel valve

(Woodward Valve) to achieve the rated power output by adjusting the engine speed. Moreover, the turbine outlet temperature is fixed at 594℃ by turbine exhaust temperature sensor (TET). The limited temperature value is set by Capstone Turbine Corporation for protecting the turbine.

The biogas consists of CH_4 and CO_2 mainly that leads to a low heating value, so the biogas inlet velocity is higher than those of the natural gas and propane for obtaining the same input heat under the same workload. Thus, the fuel injector is designed as premix type. The single premix solenoid can control fuel flow and increase flame stability when medium or low BTU content fuels are used.

In ideal state, the system of turbine engine is Brayton cycle, which has four steps. They are isentropic compression, isobaric heating, isentropic expansion and isobaric heat rejection. The theoretical thermal efficiency calculation is analyzed by Brayton cycle. Figure 3.3 shows the CR30 equipments and the following Table 3.1 shows the detailed data of engine.

Table 3.1 Engine Technical Data

Capstone Turbine Engine			
Engine model	CR30		
Electrical Power Output	30 kW		
Voltage	400 to 480 VAC		
Electrical Service	3-Phase, 4 Wire		
Maximum Engine Speed	96000 rpm		
Rated Efficiency	Compressor 0.76	Combustor 0.96	Turbine 0.84
Dimensions	0.76×1.5×1.9 m (30×60×70 in)		
Compression ratio	3.8		
Digester / Landfill Gas HHV	12.1 - 32.1 MJ/m^3 (325 – 861 BTU/scf)		
Frequency	50 / 60 Hz		
Maximum Output Current	46A, grid connect operation		
Electrical Efficiency	26 %		
Dry weight	405 kg		
Power-to-weight (specific power)	0.074 kW/kg (0.045 hp/lb)		

3.1.2 Biogas Flow Meter (TBT-FT004)

Fig 3.4 shows the mass flow transmitter, TBT-FT004, used for measuring the mass flow rate. The mass flow transmitter is used almost entirely for gas flow applications, such as compressive gas, mixed gas and unexplosive gas. The minimum length ahead the sensor along the pipe should be 10 times of pipe diameter and 5 times behind sensor for forming the fully developed flow. The principle of flow meter is thermal-mass flow, which measures fluid mass flow rate by means of the heat convected from a heated surface to the flowing fluid. It uses heat to measure flow, and then it introduces heat into the flow steam and measures how much heat dissipates using one or more temperature sensors, hence, the heated temperature sensor is controlled by power supply and the temperature difference between these two sensors have to keep constant under a fixed mass flow rate. The different mass flow rate will result in different temperature difference. Therefore, it can deduce the mass flow rate of fluid by the quantity of power supply to maintain the temperature difference between two sensors. The TBT-FT004 data are shown in Table 3.2.

Table 3.2 TBT-FT004 Flow Meter Data

Measuring object	Gas (40 ^{o}C 5.6 kgf / cm^{2}G)
Measured unit	m^3/h, $m^3/\min$, $l/\min$, $kg/\min$
Power supply	12~30 VDC, 100 mA
Range ability	300 : 1
Accuracy	±3%
Temperature Range	-30 ^{o}C ~50 ^{o}C
Max. Pressure	1.6 MPa
Scale Range	0.2~90 m^3/h
Material	SUS304

3.1.3 Dehumidifier (RD-20A)

Figure 3.5 shows the dehumidifier, GTT RD-20A, used for removing the water vapor of biogas. The maximum inlet biogas flow rate is 44 L/sec. It is pre-cooled as biogas leaves from the evaporator. The coolant in the dehumidifier is R-134a. The detailed data of RD-20A are given in the Table 3.3.

Table 3.3 RD-20A Dehumidifier Data

Dehumidifier Model	RD-20A
Inlet Temperature	80℃
Inlet Pressure	7 kg/cm^2
Air Volume Rate	2.5 Nm^3/Min
Refrigerant	R-134a
Power	220V, 1ϕHz
Horsepower	1/2 HP

3.1.4 Air Compressor (H-50)

Figure 3.6 shows the compressor (H-50). It is used to compress the biogas for complying to the pressure of preheated air, which is compressed by inner compressor. If the biogas cannot attain the need of pressure level, the control system of CR30 will shut compressor down for protecting the machine. The detailed data of H-50 are shown in the Table 3.4.

Table 3.4 H-50 Air Compressor Data

Air Compressor Model	H-50
Air Volume	0.51 m^3/Min
Rated discharge Pressure	7 kg/cm^2
Driver	5HP, 220V, 60Hz
Net Weight	322 kg

3.1.5 Gas Analyzer (ECA450)

Figure 3.7 is the gas analyzer, BACHARACH ECA 450 that is used for measuring waste gas component data, which include the concentrations of oxygen, NO_x and carbon dioxide. The measured and calculated data are shown in the following Tables 3.5 and 3.6

Table 3.5 The Measured Data of Gas Analyzer ECA450

Measured Data	
Oxygen	0.1 to 20.9%
Carbon Monoxide (hydrogen compensated)	0 to 4,000 ppm
Carbon Monoxide High	4,001 to 80,000 ppm
Nitric Oxide	0 to 3,500 ppm
Nitrogen Dioxide	0 to 500 ppm
Sulfur Dioxide	0 to 4,000 ppm
Combustibles	0 to 5% (application dependent)
Stack Temp.	-4 to 2400^{o}F (-20 to 1315^{o}C)
Primary / Ambient Temp.	-4 to 999^{o}F (-20 to 537^{o}C)
Pressure / Draft	-27.7 to 27.7 inches of Water

Table 3.6 The Calculated Data of Gas Analyzer ECA450

Calculated Data	
Combustion Efficiency	0.1 to 100.0%
Excess Air	1.0 to 250%
Carbon Dioxide (dry basis)	0 to fuel dependent maximum
NO_x	0 to 4,000 ppm
NO_x (ref. to % O_2)	0 to 17,000 ppm
CO (ref. to % O_2)	0 to 99,9999 ppm
NO (ref. to % O_2)	0 to 14,900 ppm
NO_2 (ref. to % O_2)	0 to 2,100 ppm
SO_2 (ref. to % O_2)	0 to 17,000 ppm

3.1.6 Methane Concentration Analyzer (GuardCH4)

Figure 3.8 shows guardian plus infra-red gas monitor GuardCH4, which is used for measuring the methane concentration of the inlet treated biogas.

3.1.7 Humidity Temperature Meter (Center 311)

The Center311 humidity temperature meter is shown in Fig. 3.9. It is used to measure the humidity and temperature of the environment and biogas.

3.1.8 Gas Analyzer (IR-208)

Figure 3.10 shows the IR-208 Gas Analyzer. It integrates two different types of gas measurement into one instrument. A multiple channel infrared detector array utilizing a single beam infrared optical system detects target gases using specially designed narrow band-pass optical filters. Comparing the infrared absorption of the reactive detectors to the nonreactive detector in the array provides the comparative for measuring the gas concentration in the sample stream. With a choice of more than 270 gases, up to 3 gases can be measured under infrared and up to 3 additional gases can be measured utilizing electrochemical cell, paramagnetic, or other sensors. The specification data of gas analyzer (IR-208) are shown in the following Table 3.7.

Table 3.7 The Specification Data of Gas Analyzer IR-208

Specification	Value
Measuring method	NDIR single beam
Response time	2 seconds
Pressure	5 Psig
Maximum load impedance	4-20mA isolated output 500 ohms
Power source	120/240 VAC, 50/60 Hz
Sample flow	Standard: 0.2 to 2.0 L/Min
Sample temperature	32° to 150°F (0° to 70°C)
Weight	16 lbs. (7.3kg)
Resolution	0.1 ppm
Repeatability	+ or – 0.25% of full scale

3.2 The Theoretical Calculation

The following calculations include the excess air ratio, thermal efficiency, theoretical fraction of mole of CO_2 in waste gases, the percentage of water vapor removed from biogas. These data will be used in the analysis of the following experiments.

3.2.1 Excess Air Ratio

The air-fuel ratio (AF) is defined as a ratio of mole of air to the one of fuel in the combustion process. The treated biogas contains air, which leaks from atmosphere to the storage tank when the pipe of anaerobic fermentation pool is too low. Hence, the stoichiometric reaction for combustion of biogas with standard air is given as:

$$CH_4 + xCO_2 + y(O_2 + 3.76N_2) + zH_2O + (2-y)(O_2 + 3.76N_2) \rightarrow (1+x)CO_2 + (z+2)H_2O + 7.52N_2 \quad (3.1)$$

where x, y and z are the moles of CO_2, air and water vapor in the biogas, respectively. Both x and y can be measured by instruments, and then z can be obtained from the absolute humidity (ω) of biogas. Since the water vapor is considered as an ideal gas, the percentage of vapor from biogas can be calculated as follows:

$$Mole\ Fraction\ of\ H_2O\ in\ Biogas(\%) = \frac{18}{16\alpha+44\beta+28.8\gamma}\frac{P_v}{P_{biogas}-P_v} \quad (3.2)$$

where α, β and γ are the percentages of CH_4, CO_2 in biogas and air in biogas, respectively. P_{biogas} is the pressure of biogas and P_v is the vapor pressure in biogas, which is obtained from:

$$P_v = \Phi P_g \quad (3.3)$$

where Φ is the relative humidity , measured by instrument, and P_g the saturation pressure of vapor at the same temperature. The stoichiometric air-fuel ratio, AF_{stoich} is :

$$AF_{stoich} = \frac{mole\ of\ air}{mole\ of\ CH_4 + mole\ of\ CO_2 + mole\ of\ air\ in\ biogas + mole\ of\ H_2O}$$

$$= \frac{(2-y)\times 4.76 mole}{(1+x+y\times 4.76+z) mole} \quad (3.4)$$

On the other hand, AF_{act} is the air-fuel ratio of the actual mole of the air to the summation of moles of the methane, CO_2 and air in biogas into the engine. Because the mole ratio is equal to the volume flow rate ratio, and the summation of the methane, CO_2, air and water vapor in biogas flow rate is equal to the biogas flow rate. AF_{act} can be also expressed as:

$$AF_{act} = \frac{(mole\ of\ air\ )_{act}}{(mole\ of\ CH_4 +\ mole\ of\ CO_2 + mole\ of\ air\ in\ biogas + mole\ of\ H_2O)_{act}}$$

$$= \frac{Air\ flow\ rate}{CH_4\ flow\ rate +\ CO_2 flow\ rate + air\ flow\ rate\ in\ biogas + H_2O\ flow\ rate}$$

$$= \frac{Air\ flow\ rate}{Biogas\ flow\ rate} \quad (3.5)$$

The air flow rate can be measured by air flow meter directly, whereas the methane flow rate is obtained by the measured biogas flow rate multiplied by the mole fraction of methane.

The Excess Air Ratio (λ) is the ratio of the actual mole of air used to the stoichiometric mole of air, defined as:

$$\lambda = \frac{(mole\ of\ air)_{act}}{(mole\ of\ air)_{stoich}} = \frac{(\frac{mole\ of\ air}{mole\ of\ fuel})_{act}}{(\frac{mole\ of\ air}{mole\ of\ fuel})_{stoich}} = \frac{AF_{act}}{AF_{stoich}} \quad (3.6)$$

Note that the actual mole of fuel is equal to stoichiometric mole of fuel because in the engine experiments the fuel supply rate is fixed, whereas the air volume flow rate is changed. As a consequence, the excess air ratio is equal to ratio of AF_{act} to AF_{stoich}. The λ is reciprocal of equivalence ratio. In this study, the most of air is used to cool the hot gas for protecting the blades of turbine.

3.2.2 Thermal Efficiency

The thermal efficiency is defined as the ratio of the actual power generation to the energy input, and its formula is as following:

$$Thermal\ Efficiency = \frac{Actual\ Power\ Generation}{Energy\ Input} \tag{3.7}$$

The actual power generation of this study is the net power output of turbine generator. The energy input is calculated from the lower heating value (LHV) of methane, whose value is 50020 kJ / kg. It is expressed as following:

$$Energy\quad Input = \dot{m}_{CH_4} \times LHV\ of\ CH_4 \tag{3.8}$$

where $\dot{m}_{CH_4}$ is the methane mass flow rate in biogas, and is calculated by :

$$\dot{m}_{CH_4} = \dot{V}_{biogas} \times \rho_{biogas@1atm,25°C} \times mf_{CH_4@5atm} \tag{3.9}$$

where $\dot{V}_{biogas}$ is measured biogas volumetric flow rate, $\rho_{biogas@1atm,25°C}$ is density of biogas in normal condition. $mf_{CH_4@5atm}$ is mass fraction of CH_4 in biogas at five atmospheric pressure.

3.2.3 Least Square Method

The least square method is applied to find the curve which represents the relationship between the measured data, and the curve has minimum value that the sum of the square of the distance which is all the data points to the curve. This study uses first-order linear curve to do the least square method for finding the representative curve. The equations are expressed as following:

$$f(x) = ax + b \tag{3.10}$$

$$a = \frac{\sum_{i=1}^{n} x_i \sum_{i=1}^{n} y_i - n\sum_{i=1}^{n} x_i y_i}{(\sum_{i=1}^{n} x_i)^2 - n\sum_{i=1}^{n} x_i^{\;2}} \tag{3.11}$$

$$b = \frac{\sum_{i=1}^{n} x_i y_i \sum_{i=1}^{n} x_i - \sum_{i=1}^{n} y_i \sum_{i=1}^{n} x_i^{\;2}}{(\sum_{i=1}^{n} x_i)^2 - n\sum_{i=1}^{n} x_i^{\;2}} \tag{3.12}$$

where a is slope of the line, b intercept and n the number of measured values.

In order to ensure whether the curve can represent the measured data, the goodness of fit (R^2) is a good indicator for examining the linear regression. The goodness of fit is given as following:

$$R^2 = \frac{ss_{xy}^2}{ss_{xx} \times ss_{yy}} \tag{3.13}$$

$$ss_{xx} = \sum_{i=1}^{n}(x_i - \bar{x})^2 \tag{3.14}$$

$$ss_{yy} = \sum_{i=1}^{n}(y_i - \bar{y})^2 \tag{3.15}$$

$$ss_{xy} = \sum_{i=1}^{n}(x_i - \bar{x})(y_i - \bar{y}) \tag{3.16}$$

where $\bar{x}$ and $\bar{y}$ are the average measured data.

If the R^2 is higher, the curve can represent the good tendency of measured data. When R^2 equals to 1, it is called perfect fit, meaning that the regressive model does not exist the residuals.

3.3 Waste Gas Analysis

The contents of waste gases include O_2, CO_2, CO and NO_x. The gas analyzer (IR-208) can measure the concentrations of waste gases. However, the gas turbine needs most of the air to cool the hot gas to avoid damaging the turbine. Thus, the concentration of NO_x is too low to measure by instrument.

The measured O_2 data can be applied to estimate CO_2, excess air ratio and mole number of waste gas composition. Because the cooling air is mixed with produced CO_2, the measured concentration of CO_2 is larger than actual one. Moreover, the quantity of air is much higher than CH_4 in exhaust gases, hence, the term of methane does not appear in actual reaction formula. Eq. (3.1) is modified by the excess air ratio for obtaining the actual reaction formula. Eq. (3.17) can find the concentration of CO_2 and excess air ratio by the O_2 mole fraction.

The actual reaction formula is expressed as following:

$$CH_4 + xCO_2 + y(O_2 + 3.76N_2) + zH_2O + \lambda(2-y)(O_2 + 3.76N_2) \rightarrow (y - y\lambda + 2\lambda - 2)O_2 + (2+z)H_2O + (1+x)CO_2 + 3.76(y - \lambda y + 2\lambda)N_2 \tag{3.17}$$

where x, y and z are the moles of CO_2, air and H_2O in the biogas, respectively, and λ is the excess air ratio.

The mole fraction of O_2 is applied to deduce the excess air ratio, and then the excess air ratio is used to deduce theoretical mole fraction of CO_2 in waste gases.

$$Mole\ fraction\ of\ O_2\ (\%) = \frac{y + (2-y)\lambda - 2}{1 + x + 4.76(y - \lambda y + 2\lambda) + z} \tag{3.18}$$

where $1 + x + 4.76(y - \lambda y + 2\lambda) + z$ is the total moles of waste gas and $y + (2-y)\lambda - 2$ is mole of O_2. The mole fraction O_2 is measured by instrument and the coefficient a will be found.

The percentages of CO_2 in waste gases can be calculated by:

$$Mole\ fraction\ of\ CO_2\ (\%) = \frac{1 + x}{1 + x + 4.76(y - \lambda y + 2\lambda) + z} \tag{3.19}$$

3.4 Theoretical Calculation of Performance for Micro-Gas Turbine

The theoretical calculation of performance is calculated by isentropic process and rated efficiency of component given from Table 3.1, such as compressor and turbine. The temperature and pressure points are marked in Fig. 3.11. In fact, the exit temperatures of components cannot be measured by instruments directly due to the restrictions of AIDC, hence, those above isentropic efficiencies are applied for estimating the actual temperatures of components.

η_c is the isentropic efficiency of the compressor, and η_T is isentropic efficiency of the turbine. It is expressed as:

$$\eta_C = \frac{W_{C,isen}}{W_C} \tag{3.20}$$

$$\eta_T = \frac{W_T}{W_{T,isen}} \tag{3.21}$$

where $W_{C,isen}$ is the isentropic work required by compressor, $W_{T,isen}$ is the isentropic work output by turbine, W_C is realistic work input by compressor and W_T is realistic work output by turbine. Eqs. (3.20) and (3.21) are applied for calculating the actual outlet temperature of compressor and the actual inlet temperature of turbine, respectively.

$$W_C = \frac{\dot{m}_{air} \times C_{p,air} \times (T_2 - T_1)}{\eta_{mech}} \tag{3.22}$$

$$W_T = \dot{m}_{gas} \times C_{p,gas} \times (T_4 - T_5) \times \eta_{mech} \tag{3.23}$$

$$W_{C,isen} = \dot{m}_{air} \times C_{p,air} \times (T_{2s} - T_1) \tag{3.24}$$

$$W_{T,isen} = \dot{m}_{gas} \times C_{p,gas} \times (T_{4s} - T_{5s}) \tag{3.25}$$

where η_{mech} is mechanical efficiency.

The W_{net} is the net output that work of turbine minus compressor. It is expressed as:

$$W_{net} = W_T - W_C \tag{3.26}$$

The hot gas mass flow rate that drives blades of turbine is expressed as:

$$\dot{m}_{gas} = \dot{m}_{air} + \dot{m}_{biogas} \tag{3.27}$$

where $\dot{m}_{air}$ is air mass flow rate and $\dot{m}_{biogas}$ is biogas mass flow rate. The air mass flow rate is measured by Capstone remote monitoring software and the biogas mass flow rate is obtained from:

$$\dot{m}_{biogas} = \dot{V}_{biogas} \times \rho_{biogas@1atm,25°C} \tag{3.28}$$

The specific heat capacity mixing air with biogas is expressed as:

$$C_{p,gas} = \frac{C_{p,air} \times \dot{m}_{air} + C_{p,biogas} \times \dot{m}_{biogas}}{\dot{m}_{air} + \dot{m}_{biogas}} \tag{3.29}$$

In ideal gas reversible adiabatic process, the isentropic compressor outlet temperature and turbine inlet temperature can be expressed as following:

$$T_{2s} = T_1 \times \left(\frac{P_2}{P_1}\right)^{k-1/k} \tag{3.30}$$

$$T_{5s} = \frac{T_{4s}}{(\frac{P_4}{P_5})^{k-1/k}} \tag{3.31}$$

where k is gas constant number, $\frac{P_2}{P_1}$ is expressed as r_p called pressure ratio. Due to the pressure drop, so $\frac{P_4}{P_5}$ is expressed as following:

$$\frac{P_4}{P_5} = \frac{P_2}{P_1} \times \Delta P_{recuperator} \times \Delta P_{combustor} \tag{3.32}$$

where $\Delta P_{recuperator}$ and $\Delta P_{combustor}$ are pressure drop of recuperator and combustor, respectively.

The heat exchanger effectiveness η_{HE} is calculated by:

$$\eta_{HE} = \frac{(\dot{m} \times C_P)_{air} \times (T_3 - T_2)}{(\dot{m} \times C_P)_{air} \times (T_5 - T_2)} = \frac{(\dot{m} \times C_P)_{gas} \times (T_5 - T_6)}{(\dot{m} \times C_P)_{air} \times (T_5 - T_2)} \tag{3.33}$$

The efficiency of combustion is expressed as:

$$\eta_{comb} = \frac{(\dot{m}_{gas} \times C_{p,gas} \times T_4) - (\dot{m}_{air} \times C_{p,air} \times T_{3a} + \dot{m}_{biogas} \times C_{p,biogas} \times T_{biogas})}{\dot{m}_{CH_4} \times LHV_{CH_4}} \tag{3.34}$$

The calculated heat exchanger outlet temperature (gas side) is:

$$T_6 = T_5 - \frac{\dot{m}_{air} \times C_{p,air}(T_5 - T_2) \times \eta_{HE}}{\dot{m}_{gas} \times C_{p,gas}} \tag{3.35}$$

The isentropic thermal efficiency is the ratio of the power output to the ideal heat input that is:

$$\eta_{isen} = \frac{(W_{T,isen} - W_{C,isen})}{Q_{ideal}} \tag{3.36}$$

$$Q_{ideal} = (\dot{m}_{gas} \times C_{p,gas} \times T_{4s}) - (\dot{m}_{air} \times C_{p,air} \times T_{3s} + \dot{m}_{biogas} \times C_{p,biogas} \times T_{biogas})$$

(3.37)

The calculated thermal efficiency is the ratio of the calculated power output of a device to the calculated heat input. Its formula is expressed as:

$$\eta_{th,cal} = \frac{(W_{net} \times \eta_{generator}) - W_{consumption}}{Q_{th,cal}} \quad 3.38)$$

$$Q_{th,cal} = (\dot{m}_{gas} \times C_{p,gas} \times T_{4}) - (\dot{m}_{air} \times C_{p,air} \times T_{3} + \dot{m}_{biogas} \times C_{p,biogas} \times T_{biogas})$$

(3.39)

where $Q_{th,cal}$ is the calculated heat input, $\eta_{generator}$ generator efficiency, $(W_T - W_C) \times \eta_{generator}$ generator power output, $W_{consumption}$ internal consumption of MGT.

The actual thermal efficiency ($\eta_{th,actual}$) is the ratio of the calculated output of a device to the measured heat input, its formula is expressed as:

$$\eta_{th,actual} = \frac{(W_T - W_C) \times \eta_{generator} - W_{consumption}}{Q_{th,actual}} \quad (3.40)$$

$$Q_{th,actual} = \dot{m}_{CH_4} \times LHV_{CH_4} \quad (3.41)$$

where $Q_{th,actual}$ is actual heat input.

3.5 The Effect of Varying Loads and Ambient Temperature

The power generation of the gas turbine engine is affected by main two conditions, one is operating loads and the other is ambient temperature. Thus, the thermal efficiency and power generation will be investigated in this research. The designed range of rated power output of engine is 15kW to 30 kW, and the increment of power output is 1 kW in five minutes interval under the same environmental conditions for ensuring the system in steady state. The operating load will affect the performance of engine, such as power output. Finally, the all of measured data make average to obtain the more accurate values.

The ambient temperature is an important parameter for engine performance, so it is recorded in each load. Fig. 3.12 shows the average ambient temperature of swine farm in Taichung. The temperature range of swain farm is about 17^{o}C to 30^{o}C. According to the data of CR30 given by Aerospace Industrial Development Corporation (AIDC), the net power output and electrical efficiency are affected by ambient temperature seriously. Thus, the performance of MGT affected by ambient temperature is analyzed in this research.

The experimental procedure is as follows:

1. Record ambient temperature and measure the relative humidity, temperature and pressure of treated biogas.
2. Measure the treated biogas constitutes and concentrations of methane
3. Warm up the engine at least 10 minutes in 15kW so it would be steady.
4. Record all of the measured data, such as above all and prepare all of

the instruments.

5. Adjust the power output at demanded quantity and record the net power output, biogas flow rate, air mass flow rate, and so on.
6. Repeat the procedure for different power output.
7. Repeat the above procedure at different ambient temperature.

Besides, if the ambient temperature is too low, the biogas supply will get some troubles. We check the condition of biogas before carrying out the experiment. There are two problems about biogas and they lead micro-gas turbine not to work. Firstly, the swine farm is not usually clean the swine house in the winter, otherwise, pigs may catch cold. Thus, the waste water, which flows into the anaerobic fermentation tank, is not enough to achieve the standard level of water. This situation causes the quantity of biogas to decrease. In addition, the level of water is too low (< 90 cm) that makes outside air to leak into anaerobic fermentation tank, so the concentration and quantity of biogas are affected by above reasons. Secondly, the biogas is treated by biological desulphurization system, the low temperature will cause decreasing activity of desulfurization bacteria, thus, the concentration of H_2S, which can corrode the turbine engine, increases up to 500 ppm.

3.6 Uncertainty Analysis

The accuracy of the measured data should be confirmed before the analyses of experimental results are carried out because the exactitude of the data may not be very good. Error analysis is a method applied to quantify validity and accuracy of measured data. The devices of experiment have deviation of measurement, which affects the accuracy of measured data, and other errors are from the improper operation. There are three reasons to cause these errors including instrument error, method error and artificial error. The experimental errors can be defined as determination errors and indeterminate errors. The determination errors can be called systematic errors that have constant value caused by devices themselves, so the measured values have same tendency. Furthermore, the indeterminate errors can be said random errors, which must use statistical method to solve and the values irregular.

3.6.1 Uncertainty Analysis of Mass Flow Meter

In this study, the mass flow meter is thermal mass flow meter (TBT-FT004). The disturbed flow and inside component sensors will cause the measurement deviation, the measurement range of TBT-FT004 adopted in this study is 5~2830 L/min ± 3%. The biogas flow rate is used to calculate the thermal efficiency, so the error will affect the result.

3.6.2 The Experimental Repeatability

To verify experimental accuracy, the measured data are recorded five times in each load. Then the standard deviation and coefficient of variation (CV) are applied to evaluate the accuracy of measured data. The standard deviation shows how much variation or dispersion from the average value. It is defined as:

$$S_N = \sqrt{\frac{1}{N}\sum_{i=1}^{N}(X_i - \overline{X})^2} \tag{3.38}$$

where N is number of measured value, X_i is measured value, $\overline{X}$ is average value of measured data.

The CV is a dimensionless number that can be used to show the extent of variability in relation to mean of the population. The measured data will be decided by acceptable standard. The coefficient of variation is defined as:

$$CV = \frac{S_N}{\overline{\overline{X}}} \times 100\% \tag{3.39}$$

Tables 3.8 and 3.9 list the standard deviation and coefficient of variation of experimental data. Figures 3.13, 3.14 and 3.15 show the experimental error bars at 31.4 ^{o}C. In the lower load, the variations of measured data are greater than those in the higher load. It is because when the components of CR30 work with lower efficiency, it results in the more losses greater than those in the high load. Thus, the control system needs more commands to adjust the fuel valve for maintaining the net power output, consequently, the variations are high in lower load.

Table 3.8 Experimental Repeatability for Thermal Efficiency at 31.4 ^{o}C

Net Power Output (kW)	Standard Deviation (kW)	CV (%)	Biogas Flow Rate (L/min)	Standard Deviation (L/min)	CV (%)
15.03	0.102	0.68	257.7	2.26	0.88
15.86	0.173	1.09	266.9	3.37	1.27
17.04	0.561	3.29	276.2	7.34	2.66
18.23	0.371	2.03	284.9	3.79	1.33
19.05	0.346	1.82	289.9	2.01	0.69
20.00	0.208	1.04	300.4	1.46	0.49
21.14	0.198	0.94	310.2	1.66	0.54
21.96	0.143	0.65	321.3	2.03	0.63
22.98	0.181	0.78	330.6	2.25	0.68
24.01	0.088	0.36	341.6	1.75	0.51
24.00	0.036	0.15	341.5	2.26	0.66

Table 3.9 Error Analysis for Thermal Efficiency at 31.4 ^{o}C

Net Power Output (kW)	Thermal Efficiency (%)	Standard Deviation (%)	CV (%)
15.03	15.7	0.19	1.19
15.86	16	0.14	0.86
17.04	16.6	0.80	4.85
18.23	17.3	0.45	2.64
19.05	17.7	0.33	1.85
20.00	17.9	0.25	1.37
21.14	18.4	0.24	1.32
21.96	18.4	0.12	0.64
22.98	18.7	0.21	1.14
24.01	18.9	0.15	0.79
24.00	18.9	0.14	0.77

3.6.3 CR30 System Stability

Figures 3.16 and 3.17 show the system stability in 15 and 22 kW, respectively. The data points are obtained after users increase the rated power output for analyzing stability of engine and ensuring the timing to record the data. The net power output is obtained from power meter, whose current is recorded after it is consumed by compressor (H-50) and freeze dryer (RD-20A). Therefore, the recorded power outputs are lower than the real rated power output, generated by MGT. The MGT system approaches stable after it runs for two minutes, which offers the standard of time to consult for recording those data in this study.

Chapter 4

Results and Discussion

The experimental study, a continuous effort of Ge [4], is carried out with 30kW micro-gas turbine (MGT) in a swine farm in Taichung. It is one of products of Capstone so no refit can be allowed. Note that the turbine outlet temperature is always fixed at 594 ^{o}C under any operation, assigned by Capstone. The effect of ambient temperature on engine performance is investigated with an aid of theoretical analyses. The biogas used in this research is supplied from the anaerobic tank made of red plastic bag. It is treated in advance with H_2S removal system due to the high concentration of H_2S (~5000 ppm) that will corrode the engine severely. By this process, the concentration of H_2S in biogas is decreased to 50 ppm. Furthermore, the biogas constituent concentrations at engine inlet are measured by using gas analyzers (IR-208), which can measure the concentrations of methane, oxygen, carbon dioxide and NO_x; see Section 3.1.8 for details. The contents of desulfurized biogas at each ambient temperature are shown in Table 4.1. In real situation, the biogas should not contain any O_2 after anaerobic process, however, it shows a lot of air in biogas, indicating that there are leakages from atmosphere to storage tank and biological desulphurization process. Moreover, the concentrations of biogas are 64, 51.7, 60 and 47.8% at ambient temperature 21.8, 23.5, 29.5 and 31.4^{o}C, respectively. It indicates that the content of CH_4 in the treated biogas changes day by day because such gas is not produced by an industrial process. In addition, the water vapor in biogas cannot be not removed completely even it passes through the dryer.

However, its quantity is approximated by using Eq. (3.2) in Section 3.2.1.

Table 4.1 Compositions of Biogas at Inlet of Turbine Engine at different Ambient Temperature

Ambient Temperature	CH_4 (%)	CO_2 (%)	Air (%)	H_2O (%)	Residues (%)
21.8 ^oC	64	19.3	10.42	1.3	4.98
23.5 ^oC	51.7	20.1	25.6	1.44	1.16
29.5 ^oC	60	12.73	18.37	1.44	2.36
31.4 ^oC	47.8	22.3	23.13	3.17	3.6

4.1 Theoretical Calculation of Performance for Micro-Gas Turbine Engine

Because many inlet and outlet temperatures and pressures in the MGT components cannot be measured by instruments directly, therefore, a theoretical analysis is adopted to obtain these data by incorporating with the applicable measurements. Now, the processes of MGT are approximated by Brayton cycle together with the applications of the thermodynamic isentropic efficiency and the actual component efficiencies, provided by Ref. [18].

A case of rated power output of 25kW (corresponding a maximum engine rotational speed 96,000rpm) at ambient temperature 31.4 ^oC is given to demonstrate the theoretical analysis. Figure 4.1 shows the corresponding MGT cycle. The system is assumed as in steady state, and C_ps' do not change with temperature. Then, it follows air standard cycle, internally reversible one, and the fluid is ideal gas. The locations of temperatures and mass flow rates are marked in Fig. 4.1, and the input data are shown in Table 4.2. The air, methane and biogas mass flow rates and compressor inlet and turbine outlet temperatures are measured by sensors. The other parameters are obtained from AIDC and reference [18]. It will be demonstrated next. The entire calculation procedure to determine the unknown data (not able to measure) is given in section 3.4.

As to the pressure ratio and isentropic efficiencies of compressor and turbine, they are found by using the compressor and turbine performance maps [18] under the specified corrected mass flow rate and engine speed ratio. The corrected mass flow rate is expressed as:

$$\dot{m}_{correct} = \dot{m}_{air} \times \sqrt{\frac{T_{ambient}}{T_{standard}}} \times \sqrt{\frac{P_{standard}}{P_{ambient}}} \tag{4.1}$$

where $\dot{m}_{correct}$ is corrected mass flow rate, $\dot{m}_{air}$ air mass flow rate, $T_{ambient}$ ambient temperature, $T_{standard}$ temperature at standard condition, $P_{standard}$ pressure at standard condition and $P_{ambient}$ ambient pressure.

The engine speed ratio is defined as

$$N = \frac{N_{present}}{N_{\max}} \tag{4.2}$$

where $N_{present}$ is present engine speed and $N_{\max}$ maximum engine speed of turbine engine in the experiment.

Table 4.2 The Input Data in 25kW at 31.4°C

Notation	Denotation	Values
η_C	Compressor isentropic efficiency	0.767 [18]
η_T	Turbine isentropic efficiency	0.83 [18]
η_{HE}	Heat exchanger effectiveness	0.786 [24]
$\eta_{generator}$	Generator efficiency	0.96 [18]
$\eta_{mech,C}$	Compressor mechanical efficiency	0.97 [18]
$\eta_{mech,T}$	Turbine mechanical efficiency	0.97 [18]
$\dot{m}_{air}$	Air mass flow rate	16.02 kg/min (measured)
$\dot{m}_{CH_4}$	Methane mass flow rate	0.1519 kg/min (measured)
$\dot{m}_{biogas}$	Biogas mass flow rate	0.3478 kg/min (measured)
$\dot{m}_{gas}$	Hot gas mass flow rate	16.368 kg/min (measured)
$C_{p,air}$	Air specific heat capacity at constant pressure	1.005 kJ/kg [29]
$C_{p,biogas}$	Biogas specific heat capacity at constant pressure	2.2 kJ/kg [29]
C_{p,CH_4}	Methane specific heat capacity at constant pressure	1.45 kJ/kg [29]
$C_{p,gas}$	Hot gas specific heat capacity at constant pressure	1.0145 kJ/kg [29]
r_p	Pressure ratio	3.85 [18]
T_1	Compressor inlet temperature	311.7 K (measured)
T_5	Turbine outlet temperature	866 K (measured)
LHV_{CH4}	Lower heating value of methane	50020 kJ/kg [29]

Figure 4.1 shows the calculated data based on above input data (Table 4.2). The values in green are measured temperature, the ones in red are isentropic temperatures and blue ones are actual temperatures calculated by isentropic processes and rated efficiency [18], respectively. The calculated values are summarized in Table 4.3 and the works done by turbine and required by compressor, generator power output, theoretical total input heat and thermal efficiency are presented in Table 4.4.

Table 4.3 The Calculated Temperature at 31.4 ^{o}C

Notation	Denotation	Value
T_2	Compressor outlet temperature	503 K
T_{2s}	Isentropic compressor outlet temperature	458 K
T_3	Heat exchanger outlet temperature (air)	788 K
T_{3s}	Ideal heat exchanger outlet temperature (air)	866 K
T_4	Combustor outlet temperature	1185 K
T_{4s}	Ideal combustor outlet temperature	1250 K
T_5	Turbine outlet temperature	866 K
T_{5s}	Isentropic turbine outlet temperature	866 K
T_6	Heat exchanger outlet temperature (gas)	589.2 K
T_{6s}	Isentropic heat exchanger outlet temperature (gas)	458 K

Table 4.4 The Calculated Data at 31.4 ^{o}C

Notation	Denotation	Value
W_T	Turbine output work	85.66 kW
W_C	Compressor input work	52.82 kW
$W_{generator}$	Generator power output	31.54 kW
$W_{consumption}$	MGT internal consumption	2.35 kW
Q_{ideal}	Ideal heat input	111.1 kW
$Q_{th,cal}$	Calculated heat input	113.9 kW
$Q_{th,actual}$	Actual heat input	126.7 kW
η_{isen}	Isentropic thermal efficiency	60.4 %
$\eta_{th,cal}$	Calculated thermal efficiency	25.62 %
$\eta_{th,actual}$	Actual thermal efficiency	23.04 %

Table 4.5 shows the comparison of the calculated temperatures with Capstone data at full power (96000 rpm). It indicates that the exit temperatures for each component in this research are very close to the Capstone data except the combustor outlet temperature. It is because that the adiabatic assumption is applied in combustor performance in this study that it leads to the present combustor outlet temperature is greater than the one given by Capstone.

Table 4.5 Comparison of the Calculated Temperature with Capstone data

	This Study	Capstone
Ambient Temperature T_0 (K)	304.4	288
Compressor Outlet Temperature T_2 (K)	503	478
Heat Exchanger Outlet Temperature (air side) T_3 (K)	788	783
Combustor Outlet Temperature T_4 (K)	1185	1089
Turbine Outlet Temperature T_5 (K)	865.9	866

Heat Exchanger Outlet Temperature (gas side) T_6 (K)	589.2	589

Now, this above procedure is applied to 15~30kW at ambient temperature 31.4 °C for obtaining the performance of MGT under different workload. The input data are shown in Table 4.6, and the results for each workload by using the data of Table 4.6 are shown in Table 4.7.

Table 4.6 Input Data of the Calculation in 15~30 kW at 31.4 °C

Rated Power Output (kW)	Corrected Air Mass Flow Rate (kg/s)	Engine Speed Ratio	Pressure Ratio	Compressor Efficiency	Turbine Efficiency
15	0.2276	0.892	3.15	0.753	0.845
16	0.2339	0.908	3.3	0.754	0.845
17	0.2383	0.919	3.35	0.756	0.843
18	0.2406	0.926	3.4	0.756	0.843
19	0.2463	0.940	3.52	0.757	0.843
20	0.2521	0.952	3.6	0.757	0.84
21	0.2568	0.967	3.65	0.76	0.839
22	0.2617	0.978	3.75	0.762	0.839
23	0.2670	0.986	3.8	0.764	0.835
24	0.2712	0.999	3.85	0.767	0.832
25	0.2721	0.999	3.85	0.767	0.83
26	0.2724	0.999	3.85	0.767	0.83
27	0.2723	1	3.85	0.767	0.83
28	0.2721	0.999	3.85	0.767	0.83
29	0.2732	0.9999	3.85	0.767	0.83
30	0.2720	0.999	3.85	0.767	0.83

Table 4.7 Results of the Calculation in 15~30 kW at 31.4 ^{o}C

Rated Power Output (kW)	Theoretical Input Heat (kW)	Turbine Output Work (kW)	Compressor Input Work (kW)	Generator Power Output	Theoretical Thermal Efficiency (%)
15	84.08	59.61	36.93	21.78	23.11
16	89.07	64.28	39.84	23.47	23.71
17	91.58	66.36	41.00	24.35	24.02
18	93.93	68.34	42.18	25.11	24.23
19	97.96	72.07	44.64	26.34	24.51
20	101.55	75.28	46.65	27.49	24.76
21	104.59	77.78	47.99	28.60	25.09
22	108.31	81.11	49.98	29.89	25.42
23	111.43	83.63	51.34	31.00	25.71
24	113.8	85.65	52.73	31.59	25.7
25	113.9	85.66	52.82	31.53	25.62
26	114.09	85.77	52.82	31.64	25.67
27	114.07	85.76	52.83	31.61	25.65
28	113.91	85.67	52.82	31.54	25.62
29	114.4	85.98	52.80	31.85	25.78
30	113.79	85.61	52.81	31.49	25.61

Figure 4.2 shows the actual and theoretical generator power outputs, they are almost parallel and the difference is around 5 kW. The discrepancy is attributed to that the combustor is assumed as adiabatic in calculation and the pressure drop, occurred in air passage (piping loss), does not consider as well. As expected, the theoretical powers are higher than experimental ones.

The theoretical performances of gas turbine for other ambient temperature are also calculated in order to understand its effect on power output and the related reason. The input data in Table 4.8 except the measured compressor inlet temperature (T_1) are obtained from the theoretical calculation mentioned above. The rated power outputs shown in this are selected from the maximum engine speed, 96000 rpm, at each ambient temperature.

Table 4.8 Input Data at different Ambient Temperature

Ambient Temperature (^{o}C)	21.8	23.5	29.5	31.4
Rated Power Output	27	28	25	24
Engine Speed	96044	96000	96004	96262
Pressure Ratio	3.73	3.73	3.8	3.85
Compressor Efficiency	0.77	0.77	0.767	0.767
Turbine Efficiency	0.831	0.831	0.83	0.83

The calculation results are given in Table 4.9. It shows that the combustor outlet temperature is increased with an increase of the ambient temperature. The reason is that the pressure ratio at higher ambient temperature has greater value than that at lower ambient temperature; see Table 4.8. The higher pressure ratio leads to a higher inlet temperature of combustor, causing a higher outlet temperature. Of course, the higher compressor ratio needs more input work. It indicates that decrease of power output between ambient temperatures 21.8 and 31.4 ^{o}C is around 1.48 kW due to the increased required power by compressor.

Table 4.9 Results of the Calculation at different Ambient Temperature

Ambient Temperature (^oC)	21.8	23.5	29.5	31.4
Compressor Inlet temperature T_1 (^oC) (measured)	29.3	31.6	34.9	38.7
Turbine Outlet Temperature T_5 (^oC) (measured)	593.1	593.4	592.4	593
Compressor Outlet Temperature T_2 (^oC) (calculated)	208.56	212.94	221.3	230
Combustor Inlet Temperature T_3 (^oC) (calculated)	510.81	512	513	513.3
Combustor Outlet Temperature T_4 (^oC) (calculated)	903.6	904	908.4	912.1
Turbine Output (kW) (calculated)	85.45	85.93	85.24	85.66
Compressor Input (kW) (calculated)	51.32	51.87	52.2	52.8
Fuel Consumption (kW) (calculated)	114.34	115.53	113.05	113.8
Generator Power Output (kW) (calculated)	32.77	32.6	31.7	31.5
Theoretical Thermal Efficiency (%) (calculated)	26.6	26.26	25.97	25.6

Figures 4.3 and 4.4 show the T-S and P-V diagrams for the ideal and actual cycles of the gas turbine engine at 31.4 ^oC. Those temperatures are obtained from Table 4.3. There are two useful equations developed by Gibbs equations [29] for computing the entropy change of an ideal gas.

$$Tds = dh - vdP \tag{4.3}$$

$$dh = C_p dT \tag{4.4}$$

Eq. (4.3) is derived from thermodynamic relations for a simple compressible substance. Then, Eq. (4.4) is substituted into Eq. (4.3) for obtaining Eq. (4.5):

$$ds = C_p \frac{dT}{T} - R\frac{dp}{P} \tag{4.5}$$

where C_p is average specific heat at constant pressure.

Eq. (4.5) can be applied to irreversible process because the properties of a substance depend only on the state. Thus, if it has an irreversible process taking place between the given initial and final states, Eq. (4.5) can be used to compute the entropy change of process. Integrating Eq. (4.5) and it can be written as:

$$\dot{S}_2 - \dot{S}_1 = \dot{m}(C_p \ln\frac{T_2}{T_1} - R\ln\frac{P_2}{P_1}) \tag{4.6}$$

where subscript 1 and 2 represent initial and final states, respectively.

It can be seen the maximum entropy change occurs in recuperator due to the heat gain. Besides, the pressure drop of recuperator and combustor are considered in actual situation, so we can find the pressure difference in Fig. 4.4.

4.2 Power Generation by Gas Turbine Engine

The power generation produced by turbine engine is called net power output in this study. Tables 4.10 a~d show the measured and derived data as a function of specific power output of CR30 gas turbine under four different ambient temperatures. The rated power output, net power output, air flow rate and engine speed are obtained directly from Capstone remote monitoring software provided by AIDC. Biogas flow rate is measured by thermal mass flow meter, and the thermal efficiency is derived from experimental data by using Eq. (3.7). CH_4 consumption rate is calculated directly by multiplying the biogas flow rate with concentration of biogas under the assumption of complete combustion.

Figure 4.5 shows the power consumption of the digital power controller (DPC), including pre-charge board, inverter and generator inductor, DPC power board, DPC heat sink fans and so on. It can be seen that the generator power output is higher than the net power output because part of the generator power output is consumed by control system (DPC), which needs around 2.3 kW for operation.

Table 4.10a The Measured and Derived Data as a Function of Specific

Rated Power Output of CR30 gas turbine at 21.8 ^{o}C

Biogas Constituents CH_4: 64 %, CO_2: 19.3 %, Air: 10.42 %, H_2O: 1.3 %, Residues: 4.98 %						
Rated Power Output (kW)	Net Power Output (kW)	Engine Speed (rpm)	Biogas Flow Rate (L/min)	Air Flow Rate (L/min)	CH_4 Consumption Rate (L / min)	Thermal Efficiency (%)
15	14.42	82248	142.1	10723	90.94	20.4
16	16.08	83096	148.7	10919	95.17	21.8
17	16.94	84958	154.9	11273	99.14	22
18	18.16	86298	166.4	11545	106.49	22
19	19.14	87434	178.9	11925	114.49	21.5
20	20.24	88872	189.3	12191	121.15	21.5
21	21.13	89734	198.7	12425	127.17	21.4
22	21.90	91158	202.5	12710	129.6	21.8
23	22.78	92486	208.4	13027	133.3	22
24	23.97	93458	215.5	13242	137.9	22.4
25	25.08	94388	230.4	13406	147.45	21.9
26	26.01	95306	235.8	13698	150.91	22.2
27	26.56	96044	245.5	13831	157.12	21.8
28	26.83	96016	244.1	13850	156.22	22.1
29	26.99	96072	245.4	13850	157.05	22.1
30	26.48	95990	243.9	13850	156.09	21.9

Table 4.10b The Measured and Derived Data as Function of Specific Rated Power Output of CR30 gas turbine at 23.5 ^oC

Biogas Constituents CH_4: 51.7 %, CO_2: 20.1 %, Air: 25.6 %, H_2O: 1.44 %, Residues: 1.16 %						
Rated Power Output (kW)	Net Power Output (kW)	Engine Speed (rpm)	Biogas Flow Rate (L/min)	Air Flow Rate (L/min)	CH_4 Consumption Rate (L / min)	Thermal Efficiency (%)
15	15.09	83294	215	10900	111.15	17.5
16	16.13	83932	224.3	11211.1	115.96	17.9
17	17.05	84750	230.4	11414.5	119.12	18.4
18	17.91	86072	234.2	11681.4	121.08	19.1
19	19.06	87248	237.4	12000	122.73	20
20	20.06	88116	248.7	12291.5	128.58	20.1
21	21.15	89616	257.1	12533	132.92	20.5
22	22	91008	267.5	12793.6	138.29	20.5
23	23	92250	277.7	13124.1	143.57	20.6
24	24.08	93064	287.3	13308.4	148.53	20.9
25	25.05	94536	297.7	13499.1	153.91	21
26	26.07	95148	307.1	13759.6	158.77	21.2
27	27.05	95964	313.1	14001.2	161.87	21.5
28	26.88	96000	314	13899.5	162.34	21.3
29	26.66	96000	313.5	13905.8	162.08	21.3
30	26.8	96000	312.4	13956.7	161.51	21.4

Table 4.10c The Measured and Derived Data as Function of Specific Rated Power Output of CR30 gas turbine at 29.5 ^oC

Biogas Constituents CH_4: 60 %, CO_2: 12.73 %, Air: 18.37 %, H_2O: 1.44 %, Residues: 2.36 %						
Rated Power Output (kW)	Net Power Output (kW)	Engine Speed (rpm)	Biogas Flow Rate (L/min)	Air Flow Rate (L/min)	CH_4 Consumption Rate (L / min)	Thermal Efficiency (%)
15	15.08	85638	193	11455	115.8	16.8
16	16.04	86918	206.9	11799	124.14	16.6
17	17.07	87814	215.4	11994	129.24	17
18	18.05	88270	220.3	12072	132.18	17.6
19	18.96	89720	222.8	12358	133.68	18.3
20	20.06	91048	232.2	12702	139.32	18.6
21	20.98	91842	243.7	12897	146.22	18.5
22	22.04	92828	246.6	13196	147.96	19.2
23	23.07	94142	252.1	13508	151.26	19.7
24	24.08	95346	257.1	13709	154.26	20.1
25	24.44	96004	260.2	13911	156.12	20.1
26	24.48	96016	255.8	13911	153.48	20.6
27	24.44	96216	259.5	13911	155.7	20.2
28	24.65	96238	261.8	13891	157.08	20.2
29	24.49	96044	257.5	13917	154.5	20.4
30	24.51	96004	258.2	13904	154.92	20.4

Table 4.10d The Measured and Derived Data as Function of Specific Rated Power Output of CR30 gas turbine at 31.4 ^{o}C

Biogas Constituents CH_4: 47.8 %, CO_2: 22.3 %, Air: 23.13 %, H_2O: 3.17 %, Residues: 3.6 %						
Rated Power Output (kW)	Net Power Output (kW)	Engine Speed (rpm)	Biogas Flow Rate (L/min)	Air Flow Rate (L/min)	CH_4 Consumption Rate (L / min)	Thermal Efficiency (%)
15	15.03	85898	257.7	11571.3	123.2	15.7
16	15.86	87474	266.9	11887.8	127.58	16
17	17.04	88535	276.2	12115.5	132.01	16.6
18	18.23	89191	284.9	12227.9	136.16	17.3
19	19.05	90593	289.9	12518.3	138.6	17.7
20	20	91728	300.4	12812.6	143.6	17.9
21	21.14	93128	310.2	13054.6	148.27	18.4
22	21.96	94176	321.3	13301.9	153.56	18.4
23	22.98	95030	330.6	13568.7	158.01	18.7
24	24.01	96262	342.6	13789.8	163.29	18.9
25	24	96270	341.5	13831.6	163.23	18.9
26	24.14	96270	342.5	13846	163.73	19
27	23.99	96291	343.3	13836.9	164.1	18.8
28	24.05	96287	341.6	13835.6	163.3	19
29	24.13	96286	339.1	13882.7	162.06	19.2
30	23.98	96270	338.3	13825.1	161.72	19.1

Figure 4.6 shows the net power output v.s. rated power output from 15~30kW under four different ambient temperatures. It shows that both are almost coincident until the engine speed reaches 96000 rpm in 27, 28, 25, 24 kW at 21.8, 23.5, 29.5 and 31.4 ^{o}C, respectively. After that, the maximum net power output apparently is influenced by the ambient temperature. The discrepancy between the rated and net power output becomes greater as the ambient temperature is higher.

However, when MGT achieves maximum engine rotational speed (96,000 rpm), the net power outputs of 26, 27, 28 and 30 kW rated powers at 23.5 ^{o}C are higher than those at 21.8 ^{o}C. The reason is that the CH_4 concentration of biogas is 51.7% at 23.5 ^{o}C, whereas it is 64% at 21.8 ^{o}C. When the CH_4 concentration becomes lower, MGT will automatically increases the open ratio of fuel valve (Woodward Valve) to supply more biogas for maintaining the combustion. So does the air supply. These can be seen in Tables 4.10(a) and 4.10(b). Since the engine speeds are almost maintained as constant (~96000rpm) at these rated powers, the enhanced total mass flow rate increases the net power output.

Table 4.11 lists the corresponding data at 21.8 and 31.4 ^{o}C under the maximum engine speed (96000 rpm) for the interpretation of the discrepancy between the rated and net power output.

Table 4.11 Effect of Ambient Temperature Analysis

			Discrepancy
Ambient Temperature	21.8 ℃	31.4 ℃	+9.6℃
Net power output	26.56 kW	24.01 kW	-2.55 kW (9.6%)
Biogas mass flow rate (CH_4 mass flow rate)	15 kg/h (8.35 kg/h)	20.86 kg/h (9.1 kg/h)	+5.86 kg/h (+0.75 kg/h)
Air density	1.1538 kg/m^3	1.1174 kg/m^3	-0.0364 kg/m^3 (3.2%)
Air mass flow rate	994.68 kg/h	961.2 kg/h	-33.48 kg/h
Total mass flow rate	1009.6 kg/h	982 kg/h	-27.6 kg/h (2.7%)
Pressure ratio [18]	3.73	3.85	+0.12
Turbine work (Calculated)	85.45 kW	85.66 kW	+0.21 kW
Compressor work (Calculated)	51.32 kW	52.8 kW	-1.48 kW
Recuperator heat recovery (Calculated)	84.21 kW	76.63 kW	-7.58 kW

In the table, the air density is calculated by ideal gas formula. The pressure ratio, turbine output work and compressor input work are given from Section 4.1. With the increase of ambient temperature, it can be seen that the most apparent drops are the total mass flow rate, required work of air compressor and especially the recuperator heat recovery. And the turbine works are almost invariant. From this table, the main factor is the recuperator heat recovery. Since the turbine outlet temperature is designed to be fixed, the total mass flow rate will directly affect the exhaust heat from the turbine. Also, as the ambient temperature becomes higher, the compressor ratio is higher that needs more input power and leads to a higher exit temperature, resulting in a lower heat gain from recuperator.

Figure 4.7 shows the net power output and thermal efficiency as a function of ambient temperature at 22 kW net power output (the same as rated power output), where the corresponding the engine speed does not run at the maximum value. It indicates that the net power outputs are almost invariant with ambient temperature because the MGT control system will adjust the biogas and air mass flow rate automatically to main the combustion to comply with the rated power output, as mentioned previously.

Table 4.12 shows the CH_4 mass flow rate at different ambient temperatures between 15 and 24 kW of rated power output, where the corresponding the engine speed does not run at the maximum value. It indicates that the CH_4 mass flow rate is enhanced as the ambient temperature increases, but it seems not to relate with CH_4 concentration in biogas. The reason can be explain as follows. As the ambient temperature rises, the recuperator heat recovery and total mass flow rate decrease, as mentioned above. The discrepancy of recuperator heat recovery and total mass flow rate lead the fuel valve to open larger to supply more energy to increase the engine speed for attaining the fixed turbine outlet temperature and required rated power output at higher ambient temperature. Thus, it also results in the engine speed rotating faster to reach 96000 rpm at higher ambient temperature.

Table 4.12 Methane mass flow Rate at different Ambient Temperature in 15~24 kW of Rated Power Output

Ambient Temperature	CH_4 (%)	Rated Power Output (kW)									
		15	16	17	18	19	20	21	22	23	24
		CH_4 Mass Flow Rate (kg/min)									
21.8℃	64	0.0847	0.0886	0.0923	0.0991	0.1066	0.1128	0.1184	0.1206	0.1242	0.1284
23.5℃	51.7	0.1035	0.1079	0.1109	0.1127	0.1142	0.1197	0.1237	0.1287	0.1336	0.1383
29.5℃	60	0.1078	0.1155	0.1203	0.123	0.1244	0.1297	0.1361	0.1377	0.1408	0.1436
31.4℃	47.8	0.1147	0.1188	0.1229	0.1267	0.129	0.1336	0.138	0.1429	0.147	0.152

Figure 4.8 shows the thermal efficiency increases with the decrease of ambient temperature at each rated power output. In the normal operation condition between 15 and 25kW of rated power output, the thermal efficiency increases with the rated power at ambient temperatures of 23.5, 29.5 and 31.4℃. It is because MGT operates at partial loads with inlet guide vanes partially open. The gas turbine has higher internal friction losses. On the other hand, it is keep more or less constant (21.4~22.4%) at 21.8℃, whose biogas possesses 64% of CH_4. From the Technical Reference of Capstone, CR30 can achieve the best performance corresponding to thermal efficiency 26±2% by using natural gas (~100% of CH_4) at ambient temperature 15℃. It seems to indicate that the low-cost treated biogas (low H_2S) from livestock's manure can fully utilize the gas turbine to generate power.

The conditions of waste (flue) gas can show the MGT characteristic of combustion. The excess air ratio and concentrations of constituents in waste gas, including O_2, CO_2, CO, and NO_x are given in Table 4.13. All of experimental data are measured by gas analyzers (IR-208) at 31.4 ^oC and the excess air ratio is derived from Eq. (3.17) by using Eq. (3.18), Eq. (3.19) and the measured data in Table 4.1. It indicates that the NO_x cannot be measured by instruments because its concentration is too low in waste gas. The reason is that the most of inlet air is used to cool the combustor liner and downstream hot gas that is shown schematically in Fig. 4.9 [27]. Thus, the concentration of NO_x is diluted significantly with air and the quantity of thermal NO_x is decreased. Besides, the excess air ratio decreases with an increase of net power output, and CO also has this tendency. The reason is that the combustion efficiency increases with the increase of net power output and the control system adjusts the excess air ratio automatically.

Table 4.13 The Measurements of the Waste Gas Constitutes and Concentrations at 31.4 ^{o}C

Net Power Output (kW)	Measured Values					Calculated Values
	Waste Gas Temperature (^{o}C)	O_2 (%)	CO_2 (%)	CO (ppm)	NO_x (ppm)	Excess Air Ratio
15.03	175.4	17.9	2.36	486	0	8.15
15.86	177.2	17.85	2.38	463	0	7.99
17.04	179.6	17.79	2.26	394	0	7.87
18.23	176	17.75	2.22	331	0	7.76
19.05	179	17.7	2.21	292.4	0	7.65
20.00	181.2	17.69	2.23	287.4	0	7.62
21.14	184	17.65	2.22	240.4	0	7.53
21.96	186.4	17.63	2.25	214.2	0	7.46
22.98	188.2	17.61	2.24	196.6	0	7.42
24.01	189	17.59	2.33	180.4	0	7.38
24	189.8	17.59	2.35	169.6	0	7.39

4.3 Comparisons with Other Researches

In this section, the comparisons with other experiments are made for analyzing the effect on different types of fuel by using CR30. The fuel used by Adrian Vidal et al. [19] is propane, whereas the fuel used in present study is biogas, whose constituents are varied often.

Figure 4.10 shows the comparison of the net power output with the research of Adrian Vidal et al. [19] in the same 30 kW turbine engine. The nominal power output, whose values are estimated from nominal performance curves, provided by Technical Reference of Capstone [24] is also given in this figure. It indicates that Capstone one is greater than the ones of this study and Adrian Vidal et al. [19] because it operates in an ideal situation by using high-pressure natural gas as fuel. The present measurements include Ge's [4] ones at 27.5 and 28.5 ^{o}C. It can be seen that the net power outputs in this study are larger than the ones measured by Adrian Vidal et al. [19]. The reason is given by using Table 4.14. It indicates that input heats in this study are greater. It is because the MGT in the present study uses the Woodward valve (WWV) for preventing the corrosion from H_2S, whereas the one of Ref. [19] uses smart proportion valve (SPV) [24]. The different control functions lead to the different opening ratios of fuel valves, consequently, the input heats are different. As discussed previously, the biogas has a poorer quality in combustion, MGT will automatically increases the open ratio of fuel valve to supply more biogas for maintaining the combustion. At the same ambient temperature, both of air mass flow rate are same approximately under the maximum engine speed (~96000 rpm). However, the larger biogas mass flow rate is needed to maintain the combustion in the present study, whereas the propane mass flow rate in Ref. [19] can be lower. Thus, the total (Air + fuel) mass flow rates for WWV-MGT is greater than that of SPV-MGT.

Table 4.14 Comparison of Input Heat with Adrian Vidal et al. [19] in 30kW MGT at different Ambient Temperature

Ambient Temperature	Input Heat (kW)		Net Power Output (kW)		
	This Study	Adrian Vidal et al. [19]	This Study	Adrian Vidal et al. [19]	Difference
21.8 ^{o}C	121.14	112.02	26.48	26.31	0.17(0.6%)
23.5 ^{o}C	125.34	110.59	26.8	25.78	1.02 (3.8%)
29.5 ^{o}C	120.22	105.58	24.51	23.91	0.6 (2.4%)
31.4 ^{o}C	125.5	104	23.98	23.32	0.66(2.75%)

Figure 4.11 shows the comparison of the compressor inlet temperature with Ref. [19]. Obviously, the present compressor inlet temperatures are larger. The reason is that our generator needs to produce higher power output, mentioned above, and it results in a greater heat dissipated from generator. Therefore, the inlet air absorbs more heat as it passes through the generator.

Figure 4.12 shows the comparison of thermal efficiency. It can be seen that our thermal efficiency is lower than that of Adrian Vidal et al. [19]. It is because the biogas has a poorer quality in combustion, and it has to input more biogas for maintaining the net power output. Thus, the thermal efficiency is decreased. Moreover, with the ambient temperature increasing, our thermal efficiency decreases rapidly. At 31.4 ^{o}C of ambient temperature, the CH_4 concentration of biogas is 48%, which is lower than others. According to the Somehsaraei's [21] study, it confirms that the lower CH_4 concentration of biogas, the smaller thermal efficiency.

The net power output and electric efficiency are in a linear relationship obviously, thus, they can be predicted for consultation by using least square method, given in section 3.2.3. Figures 4.13 and 4.14 show the results by using the least square fit technique. The equations are expressed as following:

- **Net Power Output**

This study:

$$P = 33.165 - 0.291T \quad , \quad R^2 = 0.9548 \quad , \quad 21.8^\circ C \le T \le 32^\circ C$$

Adrian Vidal et al. [19]:

$$P = 33.121 - 0.3122T \quad , \quad R^2 = 0.985 \quad , \quad 24.4^\circ C \le T \le 28.9^\circ C$$

- **Electric Efficiency**

This study:

$$E = 0.2789 - 0.0027T \quad , \quad R^2 = 0.9316 \quad , \quad 21.8^\circ C \le T \le 32^\circ C$$

Adrian Vidal et al. [19]:

$$E = 0.2645 - 0.00135T \quad , \quad R^2 = 0.9781 \quad , \quad 24.4^\circ C \le T \le 28.9^\circ C$$

where P is net power output, E net electric efficiency, T ambient temperature and R^2 goodness of fit. The applied range of ambient temperature is between 21.8 ^{o}C and 32 ^{o}C in this study, whereas the one of

Adrian Vidal et al. [19] is between 24.4^{o}C and 28.9^{o}C (typical Mediterranean Temperature).

Our goodness of fit (R^2) is a litter worse than that of Adrian Vidal et al. [19] due to the fewer experimental data points. However, they select more accurate data by rejecting deviated ones from Fig. 4.10. The other reason is that the concentration of CH_4 in biogas is variable often, thus, the measured data possesses the larger variations, causing the smaller goodness of fit (R^2).

4.4 Economic Analysis

In this section, the annual economic benefits are investigated by the measured data. This estimation can show the annual potential of biogas generated by over 1000 pigs and consider whether it is worth to build the power plant in different scale of swine farm by using gas turbine engine and piston engine.

The benefit consider the electricity generation sole, it can be calculated by:

$$\text{Benefit}=\text{Electricity Generation}\times\text{Electricity purchase price per kWh} \tag{4.7}$$

From the study of Lin [1], the average biogas production is around 0.078m^3 per pig per day. The energy produced by turbine engine is 1.57 kWh per m^3 biogas, which is based on the data in Table 4.10, whereas the one generated by piston engine is 1.7 kWh per m^3 biogas [3]. Apparently, piston engine is more efficient in the scale of 30kW power generation.

The electricity price purchased by Taiwan Power Company is 3.2511 NT$ per kWh in 2014 [25]. The total biogas production is given by Table 4.15, obtained from Council of Agriculture Executive [26]. Then, the annual benefits using gas turbine engine and piston engine are estimated in Table 4.16 under the assumption that the biogas is fully utilized by generator. It indicates that the potential of biogas is very high. For the gas turbine, the electricity income is almost up to 600 million NT$ per year, and it has CO_2 emission reduction around 5 million tons. However, it also shows the piston engine has higher energy production, so its electricity income is greater.

Table 4.15 Statistics on Swine Farms over 1000 pigs in Taiwan [26]

Scale of Swine Farm (pigs)	Numbers of swine farm	Numbers of pig
1000 ~ 1999	1,119	1,547,809
2000 ~ 2999	229	553,659
3000 ~ 4999	149	563,044
5000 ~ 9999	82	570,663
10000 ~ 19999	38	539,749
> 20000	12	297,857
Total	1,629	4,072,781

Table 4.16 Annual Economic Benefits Using Gas Turbine Engine and Piston Engine

	Biogas Consumption (m^3/year)	Electricity Generation (kWh/year)	Electricity Income (NT$/year)	CO_2 Emission Reduction (tons)
Turbine Engine	115,952,075	182,044,758	591,845,712	2,645,800
Piston Engine	115,952,075	197,118,527	640,852,045	2,645,800

Based on the test data in this study and the measured data of Wu [3], the economic benefits of the 5,000 and 20,000-pig swine farm using both generators can be estimated and summarized in the Tables 4.17~4.20. In order to protect the piston engine, it only operates 20 hours a day. Thus, the estimations are based on that both generators operate 20 hours a day for the fair comparison. In fact, the turbine engine can operate 24 hours a day. The maximum operation scale of current biological desulphurization system now is applied the 5,000-pig swine farm, so the benefits can be estimated for present power generation system using both of generators. Besides, the scale of swine farm in Taichung is 20,000 pigs in this study. Thus, its benefits are also estimated.

Tables 4.17 and 4.18 show the electricity incomes using both generators for 5,000 and 20,000 pigs of swine farm per year. It can be seen that the electricity income by piston engine is larger than one by turbine engine because the piston engine has higher thermal efficiency. Therefore, the piston engine can reduce more CO_2 emission.

Table 4.17 Electricity Incomes for 5,000 Scale of Swine Farm per year Using Turbine Engine and Piston Engine

	Turbine Engine	Piston Engine
Numbers of Generator	1	1
Biogas Consumption	105,200 m^3/year	113,900 m^3/year
Electricity Generation	165,200 kWh/year	193,600 kWh/year
Electricity Income	537,000 NT$/year	629,400 NT$/year
CO_2 Emission Reduction	725 tons	1,175 tons

Table 4.18 Electricity Incomes for 20,000 Scale of Swine Farm per year Using Turbine Engine and Piston Engine

	Turbine Engine	Piston Engine
Numbers of Generator	5	5
Biogas Consumption	526,000 m^3/year	569,400 m^3/year
Electricity Generation	826,000 kWh/year	968,000 kWh/year
Electricity Income	2,685,000 NT$/year	3,147,000 NT$/year
CO_2 Emission Reduction	3,600 tons	5,800 tons

The payback period (N) according to Ref. [30] is an important index for benefits of power plant. It is used for evaluating how long can recover investment cost. It is expressed as:

$$N = \frac{Total\ cost}{Benefit} \tag{4.8}$$

where the total costs are shown in Tables 4.119 and 4.20, respectively. The benefit is obtained from Eq. (4.7). The annual depreciation expense applies with straight-line method [30]. The formula is expressed as:

$$\text{Annual depreciation expense} = \frac{Equipment\ cost - Residual\ value}{N'} \tag{4.9}$$

where N' is applicable life of equipment.

Tables 4.19 and 4.20 show the capital costs using both generators for

5,000 and 20,000-pig swine farm. It can be seen that the payback period and cost of electricity of gas turbine are higher than those of piston engine. It is because that the turbine engine's equipment cost is much higher than one of piston engine. Consequently, the above estimations indicate the economic benefits of piston engine are greater. However, it is true for 30 kW engine. If the generation power of engine becomes large, such as 60 kW and 200kW, then the statement may be reversed.

Table 4.19 Capital Cost for 5,000 Scale of Swine Farm per year Using Turbine Engine and Piston Engine

	Turbine Engine	Piston Engine
Numbers of Generator	1	1
Equipment Cost (Power generation system)	4,500,000 NT$	3,000,000 NT$
Electricity Bill	40,000 NT$/year	30,000 NT$/year
Maintenance Cost	94,000 NT$/year	140,000 NT$/year
Personnel Cost	110,000 NT$/year	110,000 NT$/year
Depreciation Cost	293,000 NT$/year	1954,000 NT$/year
Payback Period	15.36 year	8.6 year
Cost of Electricity	3.25 NT$/kWh	2.45 NT$/kWh

Table 4.20 Capital Cost for 20,000 Scale of Swine Farm per year Using Turbine Engine and Piston Engine

	Turbine Engine	Piston Engine
Numbers of Generator	5	5
Equipment Cost (Power generation system)	22,500,000 NT$	15,000,000 NT$
Electricity Bill	200,000 NT$/year	150,000 NT$/year
Maintenance Cost	470,000 NT$/year	560,000 NT$/year
Personnel Cost	110,000 NT$/year	110,000 NT$/year
Depreciation Cost	1,465,000 NT$/year	953,000 NT$/year
Payback Period	11.81 year	6.45 year
Cost of Electricity	2.72 NT$/kWh	1.85 NT$/kWh

Chapter 5

Conclusions and Recommendations

5.1 Conclusions

This research carries out with 30 kW micro-gas turbine engine (MGT) in a swine farm in Taichung. The performance of MGT is tested with varying load (15~30 kW) and at different ambient temperature (15~35 ^{o}C). The concentrations of component and constitutes of waste gas are measured by gas analyzers. Because many inlet and outlet temperatures and pressures in the MGT components cannot be measured by instruments directly, therefore, a theoretical analysis is adopted to obtain these data by incorporating with the applicable measurements. Then, the net power output and thermal efficiency are analyzed by measured data. After that, the comparisons with other research [19] are made. Finally, the economic benefits estimated by experimental data are based on the TPC present electricity purchase charge which is 3.2511 NT$ in 2014. Besides, the annual benefits of biogas potential and swine farm which is in different scale are analyzed and compared with piston engine.

According to above experiment and theoretical results, this study can obtain the following conclusions:

1. The theoretical calculation is based on Brayton cycle and air standard cycle. The results showed that the theoretical thermal efficiency is 25.62 %, generator power output is 31.54 kW in 25 kW of rated power output at 31.4 ^{o}C.
2. According to theoretical calculation, the combustor outlet temperature is increased with an increase of the ambient temperature. The reason is

that the pressure ratio at higher ambient temperature has greater value than that at lower ambient temperature. The higher pressure ratio leads to a higher inlet temperature of combustor, causing a higher outlet temperature. Of course, the higher compressor ratio needs more input work. It indicates that decrease of power output between ambient temperatures 21.8 and 31.4 ^{o}C is around 1.48 kW due to the increased required power by compressor.

3. Net power output and Rated power are almost coincident until the engine speed reaches 96000 rpm in 27, 28, 25, 24 kW at 21.8, 23.5, 29.5 and 31.4 ^{o}C, respectively. After that, the maximum net power output apparently is influenced by the ambient temperature. The discrepancy between the rated and net power output becomes greater as the ambient temperature is higher.
4. The net power outputs are almost invariant with ambient temperature at 22 kW net power output (the same as rated power output), where the corresponding the engine speed does not run at the maximum value. It is because the MGT control system will adjust the biogas and air mass flow rate automatically to main the combustion to comply with the rated power output.
5. The CH_4 mass flow rate is enhanced as the ambient temperature increases, but it seems not to relate with CH_4 concentration in biogas at different ambient temperatures between 15 and 24 kW of rated power output, where the corresponding the engine speed does not run at the maximum value. The reason can be explain as follows. As the ambient temperature rises, the recuperator heat recovery and total mass flow rate decrease. The discrepancy of recuperator heat recovery

and total mass flow rate lead the fuel valve to open larger to supply more energy to increase the engine speed for attaining the fixed turbine outlet temperature and required rated power output at higher ambient temperature. Thus, it also results in the engine speed rotating faster to reach 96000 rpm at higher ambient temperature.

6. In the normal operation condition between 15 and 25kW of rated power output, the thermal efficiency increases with the rated power at ambient temperatures of 23.5, 29.5 and 31.4 ^{o}C. It is because the MGT operates at part loads with inlet guide vanes partially open. The gas turbine has higher internal friction losses. On the other hand, it is keep more or less constant (21.4~22.4%) at test of 21.8℃, whose biogas possesses 64% of CH_4. From the Technical Reference of Capstone, CR30 can achieve the best performance corresponding to thermal efficiency 26±2% by using natural gas (~100% of CH_4) at ambient temperature 15 ^{o}C. It seems to indicate that the low-cost treated biogas (low H_2S) from livestock's manure can utilize the gas turbine to generate power.
7. The type of fuel affects the operation of MGT. The net power outputs in this study are larger than the ones measured by Adrian Vidal et al. [19]. It is because the MGT in the present study uses the Woodward valve (WWV) for preventing the corrosion from H_2S, whereas the one of Ref. [19] uses smart proportion valve (SPV) [24]. The different control functions lead to the different opening ratios of fuel valves, consequently, the input heats are different. The biogas has a poorer quality in combustion, MGT will automatically increases the open

ratio of fuel valve to supply more biogas for maintaining the combustion. At the same ambient temperature, both of air mass flow rate are same approximately under the maximum engine speed (~96000 rpm). However, the larger biogas mass flow rate is needed to maintain the combustion in the present study, whereas the propane mass flow rate in Ref. [19] can be lower. Thus, the total (Air + fuel) mass flow rates for WWV-MGT is greater than that of SPV-MGT.

8. Annual economic benefits indicate that the electricity income is almost up to 600 million NT$ per year, and it has CO_2 emission reduction around 5 million tons by gas turbine. However, it also shows the piston engine has higher energy production, so its electricity income is greater.
9. For 5,000 and 20,000 pigs of swine farm per year. The economic benefits by piston engine are larger than ones by turbine engine because the piston engine has higher thermal efficiency. Therefore, the piston engine can reduce more CO_2 emission. However, it is true for 30 kW engine. If the generation power of engine becomes large, such as 60 kW and 200kW, then the statement may be reversed.

5.2 Recommendations

1. Test the performance and evaluate the benefits of larger installed capacity of gas turbine engine (C65 or C200 MGT).

2. Consider the benefits and decide whether install an inlet air cooling system to enhance the power output generated by MGT.

References

[1] Wei-Tsung Lin, “A Research for Electricity Generation by Using Biogas from Swine Manure for a Farm Power Requirement”, June 2010.

[2] Sheng-Rung Huang, “The Experimental Study on Biogas Power Generation Enhanced by Using Waste Heat to Preheat Inlet Gases”, June 2011.

[3] Lin-Yu Wu, “The Experimental Study on Combustion Stability and Performance of Biogas Power Generation by Changing Spark Timing”, June 2012.

[4] Tai-chuan Ge, “Experimental Study for Power generation by Turbine Using Biogas in a swine Farm”, June 2013.

[5] Stijn Cornelissen, Michele Koper, Yvonne Y. Deng, “The role of bioenergy in a fully sustainable global energy system”, Biomass and Bioenergy, 41, pp.21-33, 2012.

[6] Wen-Tien Tsai, Che-I Lin, “Overview analysis of bioenergy from livestock manure management in Taiwan”, Renewable and Sustainable Energy Reviews, 13, pp. 2682-2688, 2009

[7] Jung-Jeng Su, Bee-Yang Liu, Yuan-Chie Chang, “Emission of greenhouse gas from livestock waste and wastewater treatment in Taiwan”, Agriculture Ecosystems and Environment, 95, pp. 253-263, 2003.

[8] Firdaus Basrawi, Takanobu Yamada, Kimio Nakanishi, Soe Naing, “Effect of ambient temperature on the performance of micro gas turbine with cogeneration system in cold region”, Applied Thermal

Engineer, 31, pp.1058-1067, 2011.

[9] Do Won Kang, Tong Seop Kim, Kwang Beom Hur, Jung Keuk Park, “The effect of firing biogas on the performance and operating characteristics of simple and recuperative cycle gas turbine combined heat and power system”, Applied Energy, 93, pp.215-228, 2012.

[10] Ashley De Sa, Sarim Al Zubaid y, “Gas turbine performance at varying ambient temperature”, Applied Thermal Engineering, 31, pp.2735-2739, 2011.

[11] Hasan Huseyin Erdem, Suleyman Hakan Sevilen, “Effect of ambient temperature on the electricity production and fuel consumption of a simple cycle gas turbine in Turkey”, Applied Thermal Engineering, 26, pp.320-326, 2006.

[12] Jean-Pierre Bedecarrats, Francoise Strub, “Gas turbine performance increase using an air cooler with a phase change energy storage”, Applied Thermal Engineering, 29, pp.1166-1172 , 2009.

[13] Takanobu Yamada, Mohamad Firdaus Bin Basrawi, Kimio Nakanishi, Hideaki Katsumata, “Analysis of the performances of biogas-fuelled micro gas turbine cogeneration systems (MGT-CGSs) in middle- and small-scale sewage treatment plants: Comparison of performances and optimization of MGTs with various electrical power outputs”, Energy, energy, 38, pp.291-304, 2012.

[14] Di-Han Wu, Chiun-Hsun Chen, “Performance Simulation Analysis on Low-heating-value Fuel Acceptability of a Micro Gas Turbine

Annular Combustor Operation”, Thesis of National Chiao Tung University, June 2007.

[15] Firdaus Basrawi, Takanobu Yamada, Shin’ya Obara, “Theoretical analysis of performance of a micro gas turbine co/trigeneration system for residential buildings in a tropical region”, Energy and Buildings, 67, pp.108-117, 2013.

[16] Jong Jun Lee, Mu Sung Jeon, Tong Seop Kim, “The influence of water and steam injection on the performance of a recuperated cycle microturbine for combined heat and power application”, Applied Energy, 87, pp.1307-1316, 2010.

[17] Naeim Farouk, Liu Sheng, Qaisar Hayat, “Effect of Ambient Temperature on the Performance of Gas Turbines Power Plant”, International Journal of Computer Science Issues, 10, 2013.

[18] Diamantis P. Bakalis, Anastassios G. Stamatis, “Full and part load exergetic analysis of a hybrid micro gas turbine fuel cell system based on existing components”, Energy Conversion and management, 64, pp.213-221, 2012.

[19] Adrian Vidal, Joan Carles Burno, Roberto Best, Alberto Coronas, “Performance characteristics and modelling of a micro gas turbine for their integration with thermally activated cooling technologies”, International Journal of Energy Research, pp.119-134, 2007.

[20] Leszek Malinowski, Monika Lewandowska, “Analytical model-based energy and exergy analysis of a gas microturbine at part-load operation”, Applied Thermal Engineering, 57, pp.125-132, 2013.

[21] Homam Nikpey Somehsaraei, Mohammad Mansouri Majoumerd,

Peter Breuhaus, Mohsen Assadi, "Performance analysis of a biogas-fueled micro gas turbine using a validated thermodynamic model", Applied Thermal Engineering, 66, pp.181-190, 2014.

[22] 2013 bp statistical review of world energy. Available: http://www.bp.com/en/global/corporate/about-bp/energy-economics/statistical-review-of-world-energy-2013.html, 2013.

[23] Bureau of energy, Ministry of Economic Affairs. Available: http://web3.moeaboe.gov.tw/ECW/populace/content/ContentLink.aspx?menu_id=137&sub_menu_id=358, 2013.

[24] Capstone Document Library. Available: http://docs.capstoneturbine.com/login.asp.

[25] Taiwan Power Company. Available: http://www.taipower.com.tw/

[26] Council of Agriculture Executive. Available: http://www.coa.gov.tw/show_index.php.

[27] H. Lefebvre and Dilip R., Ballal, Third Edition, Gas Turbine Combustion, CRC Press, Boca Raton, 2010.

[28] Boyce and Meherwan P., Fourth Edition, Gas turbine engineering handbook, Elsevier Inc., Waltham, 2011.

[29] Sonntag et al., Fifth Edition, Fundamentals of Thermodynamics, JOHN WILEY & SONS, INC., New York, 1998.

[30] Chan S. Park, Fourth Edition, Engineering Economics, Pearson Prentice Hall, New Jersey, 2007.

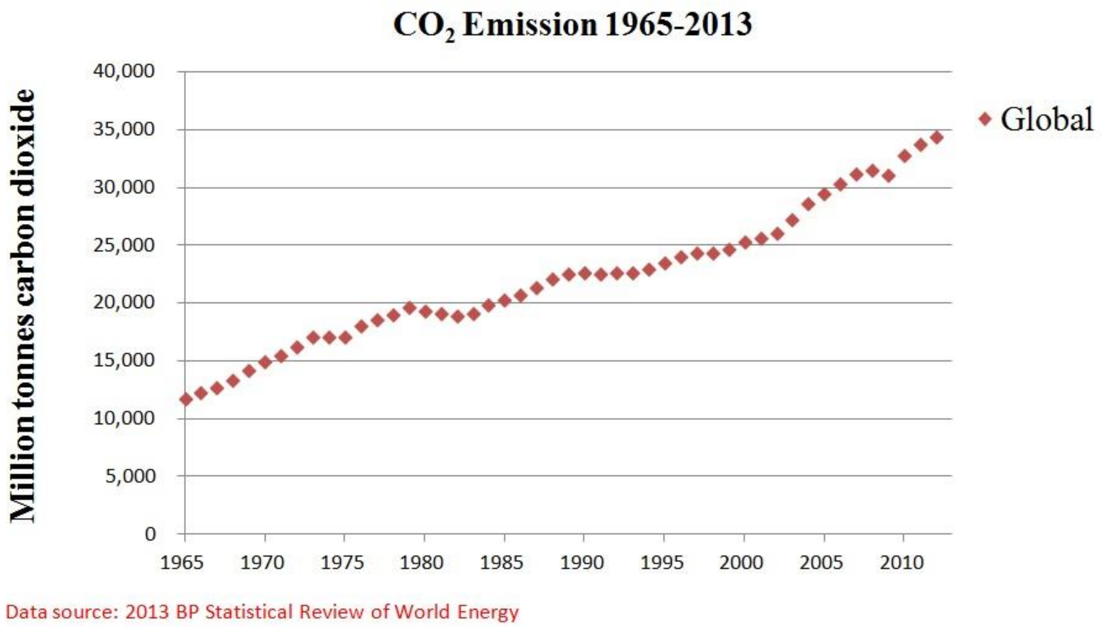

Figure 1.1 Carbon Dioxide Emission [22]

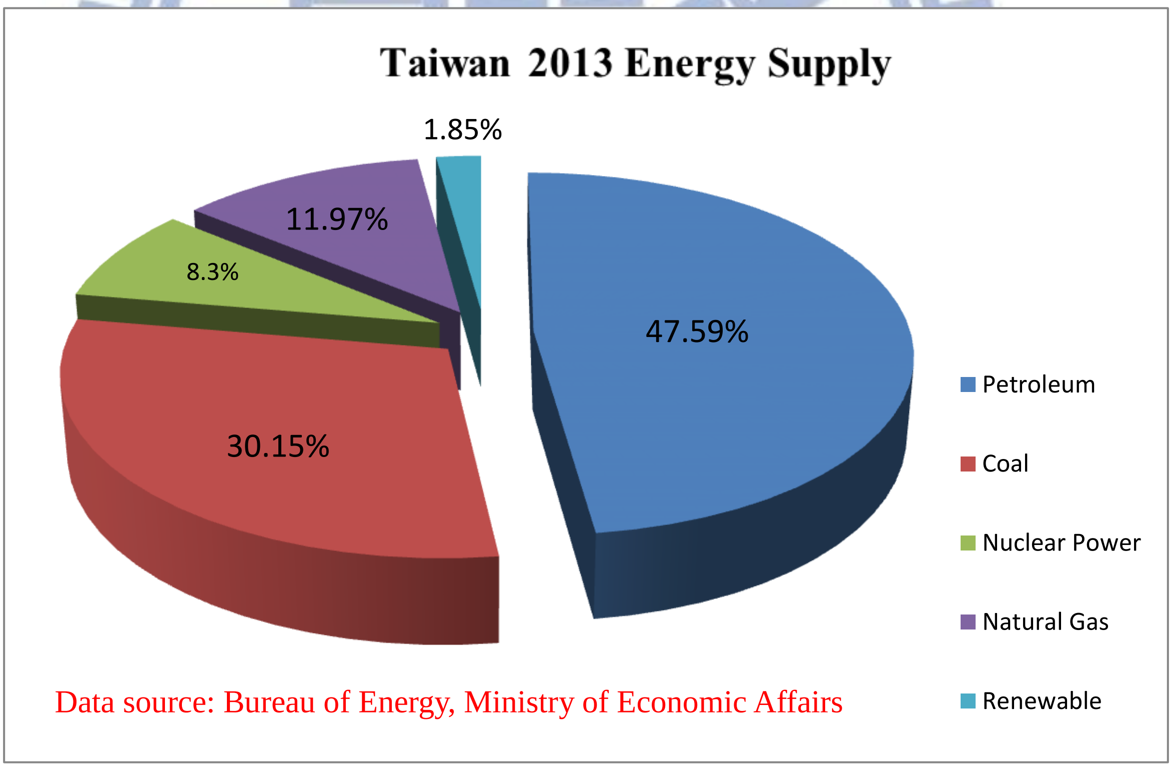

Figure 1.2 Energy Supply in Taiwan [23]

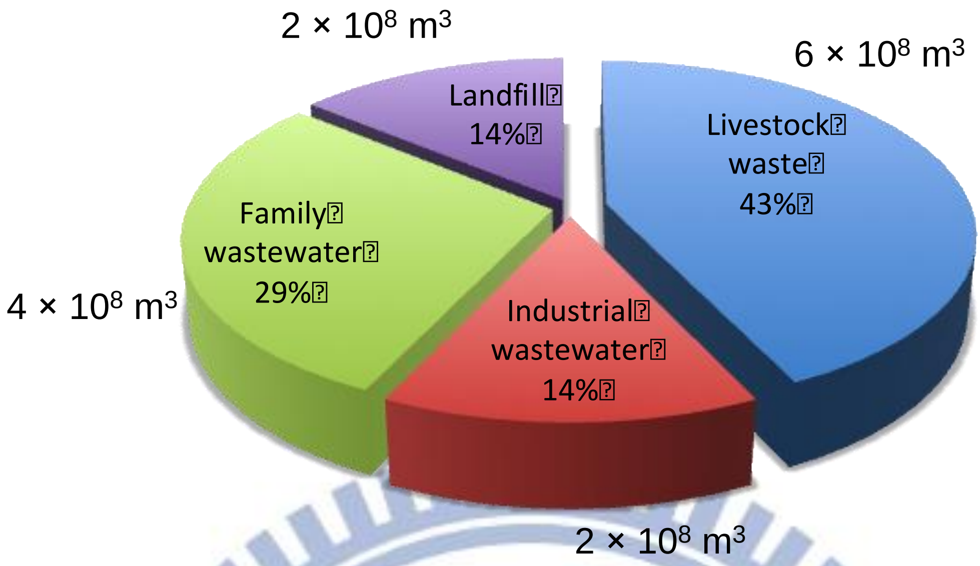

Figure 1.3 Biogas Potential in Taiwan

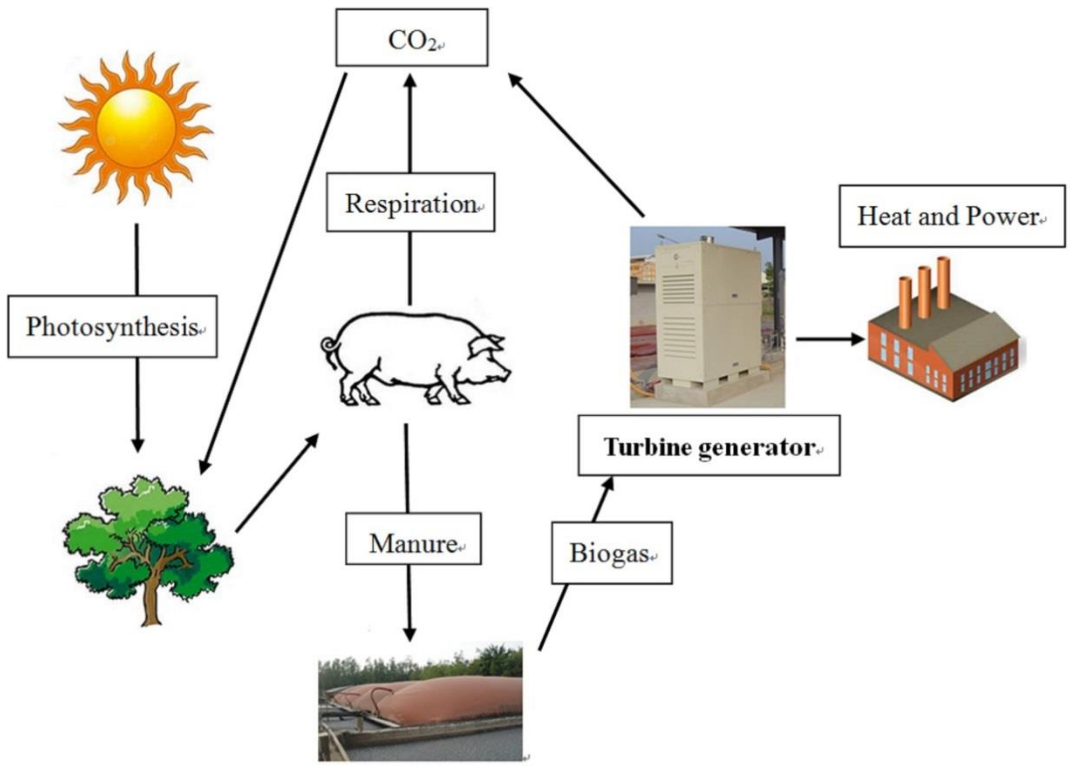

Figure 1.4 Simple Carbon Cycle for Biogas

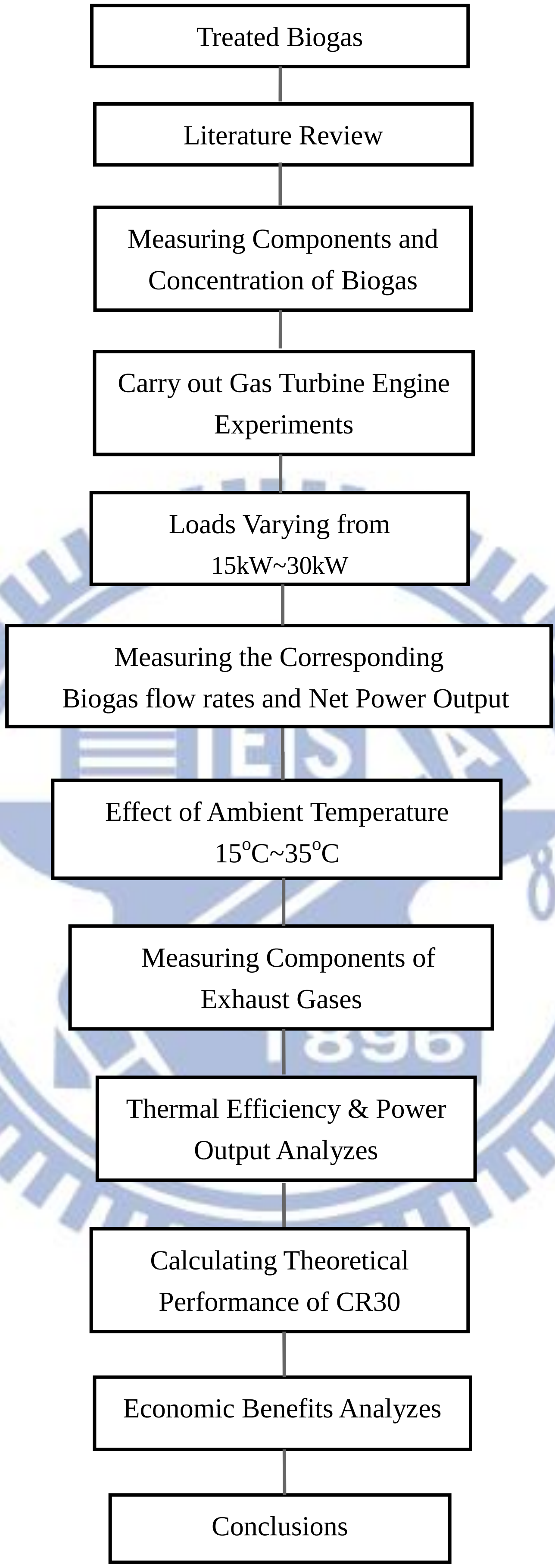

Figure 1.5 Scope of this Research

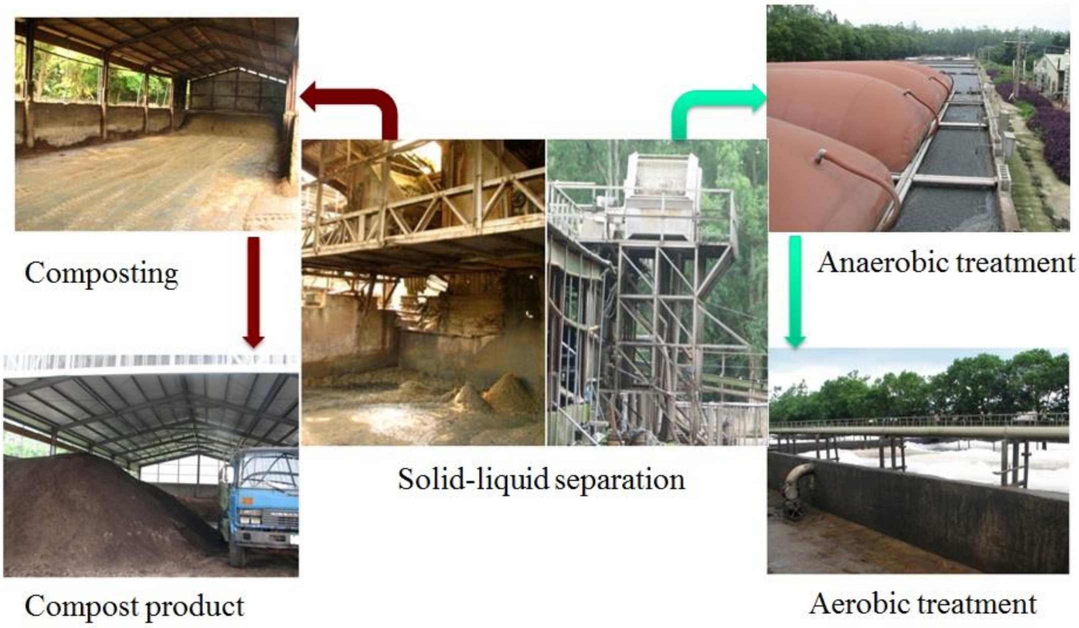

Figure 2.1 Three-Stage Wastewater Treatment in Taiwan

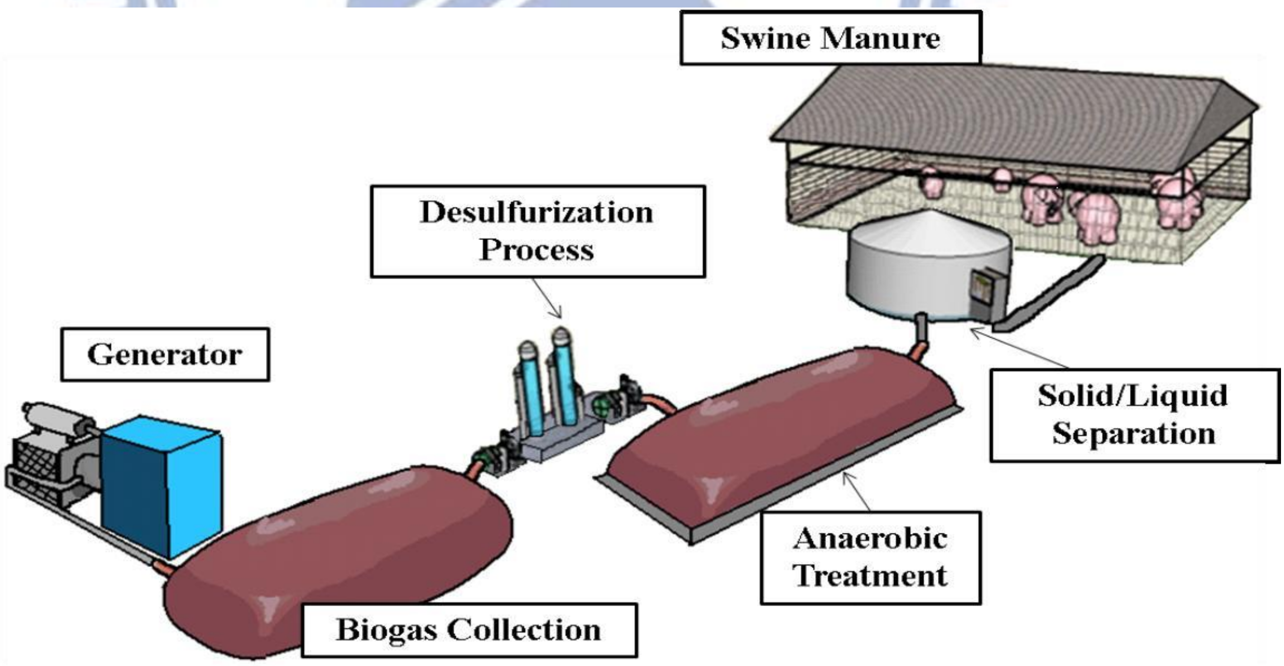

Figure 2.2 Process of Biogas Production

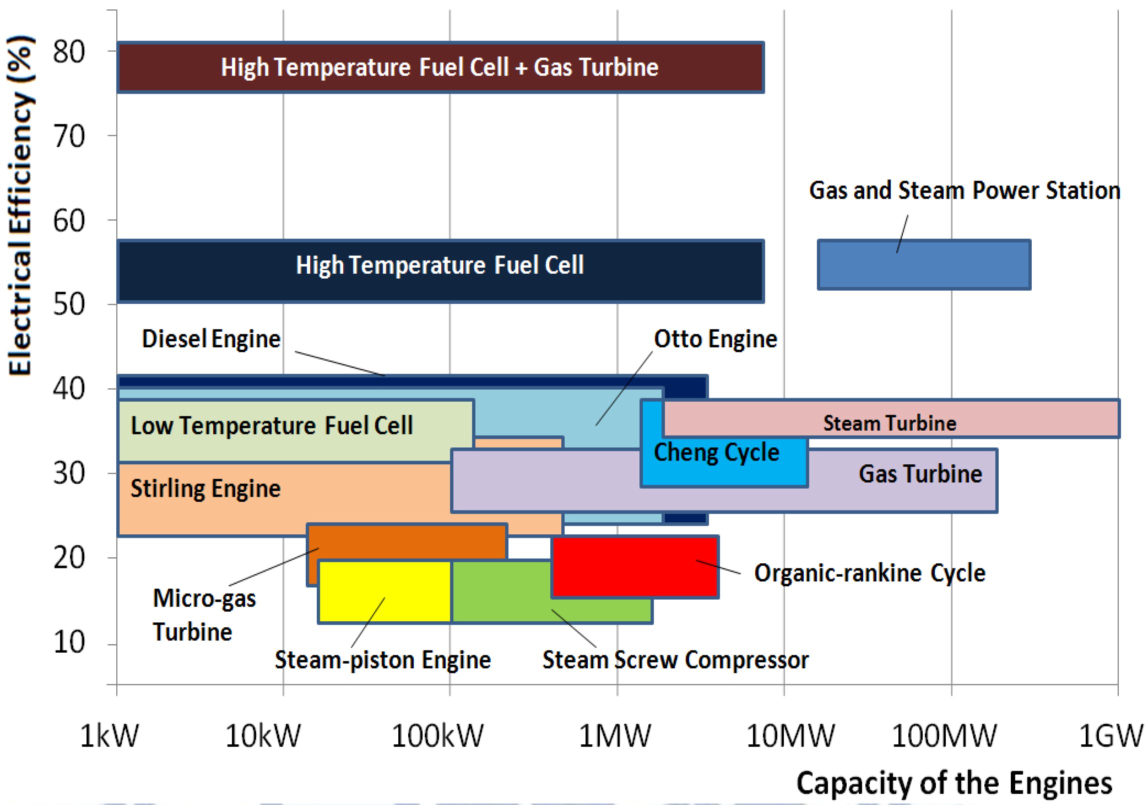

Figure 2.3 Range of Capacities for the Power Generators

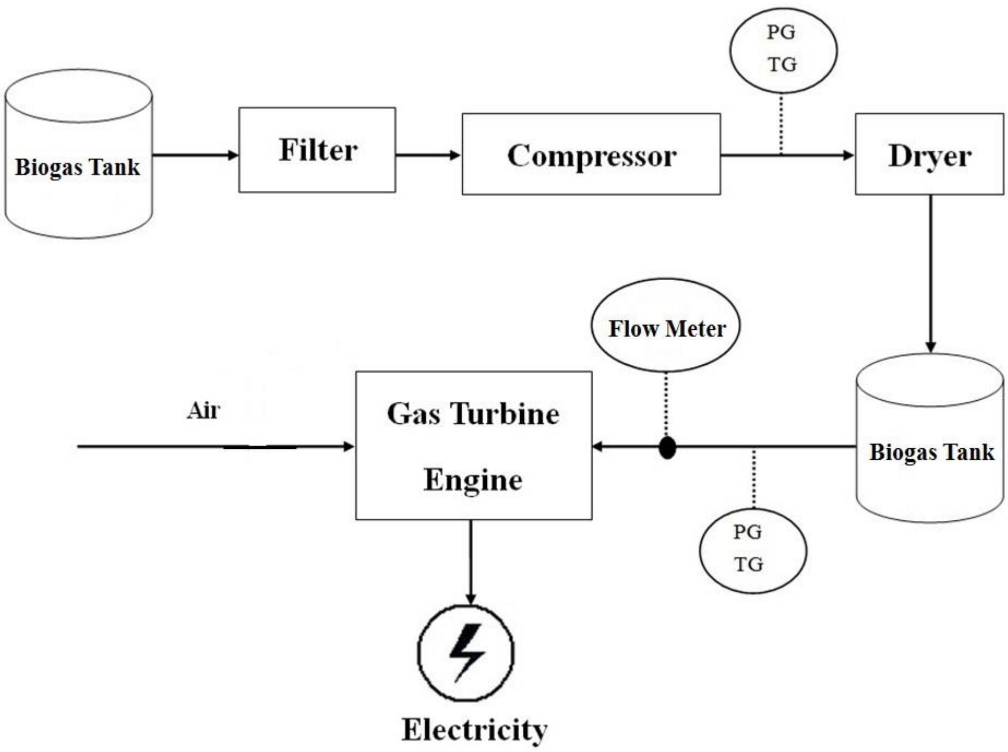

Fig. 3.1 Experiment Layout & Biogas Pretreatment System

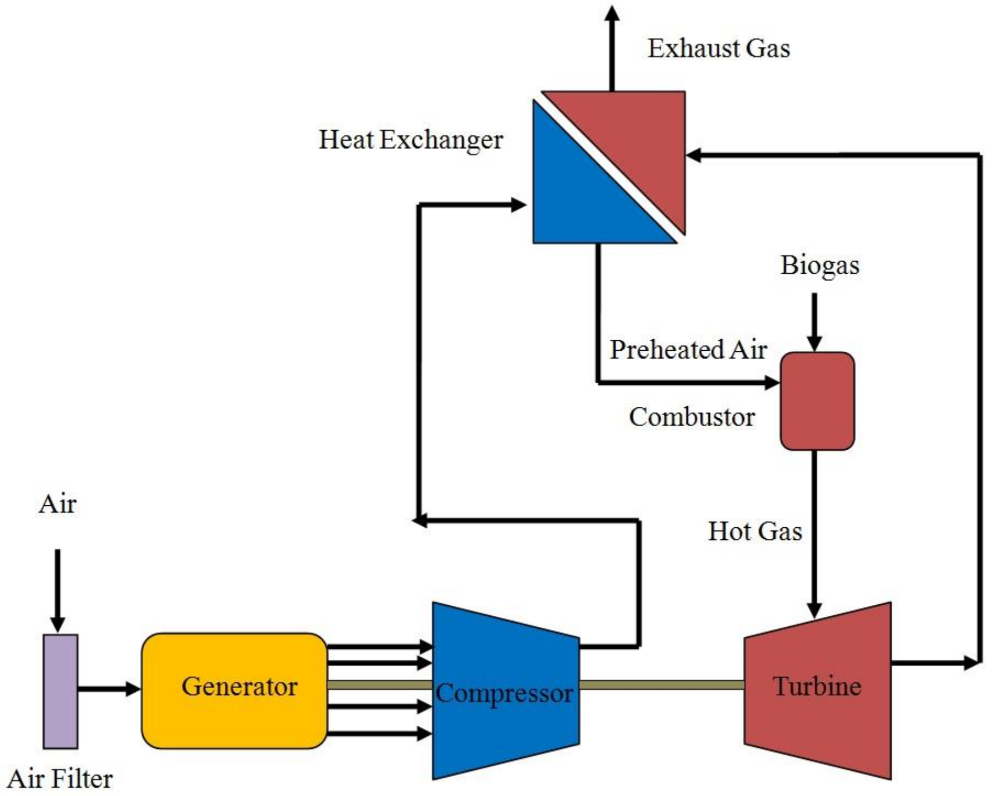

Fig. 3.2 Schematic Procedure of Micro-Gas Turbine Engine

Fig. 3.3 CR30 Micro Turbine Engine

Figure 3.4 TBT-FT004 Flow Meter

Figure 3.5 Dehumidifier (RD-20A)

Figure 3.6 Air Compressor (H-50)

Figure 3.7 Gas Analyzer (ECA450)

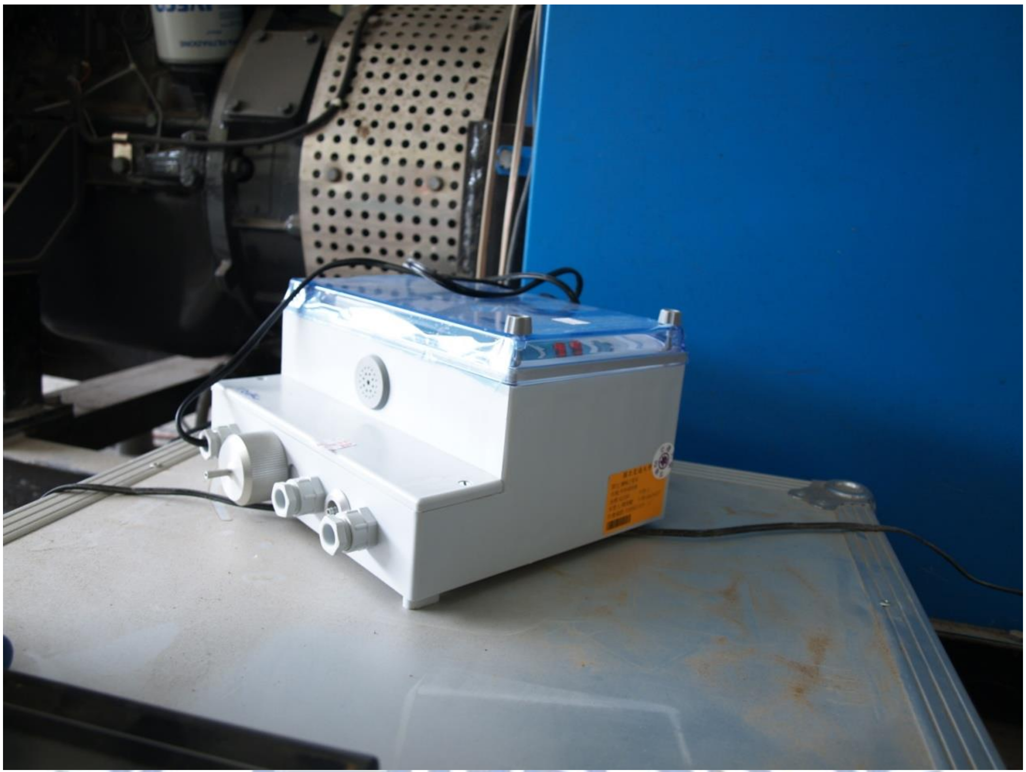

Figure 3.8 Guardian Plus Infra-Red Gas Monitor

Figure 3.9 Humidity Temperature Meter (Center 311)

Figure 3.10 Gas Analyzer (IR-208)

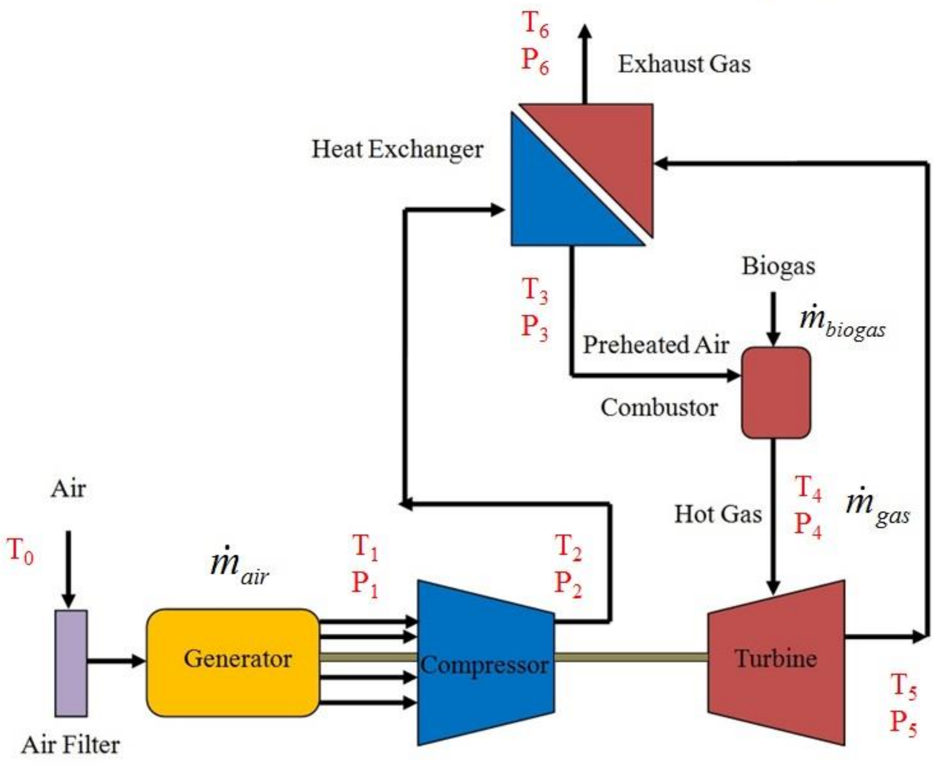

Figure 3.11 The Marked Temperature for Theoretical Thermal Efficiency

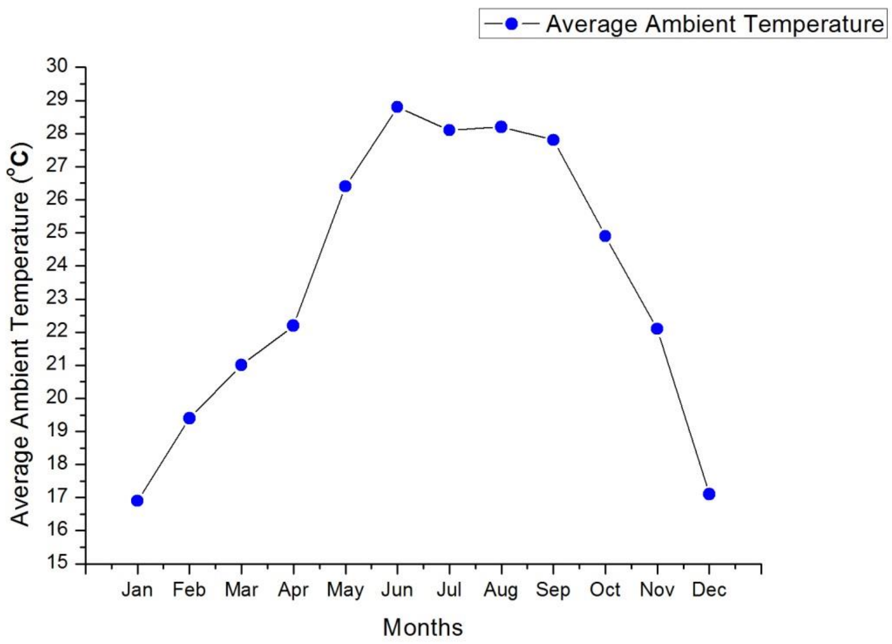

Figure 3.12 Ambient Temperature in Different Months in Taichung

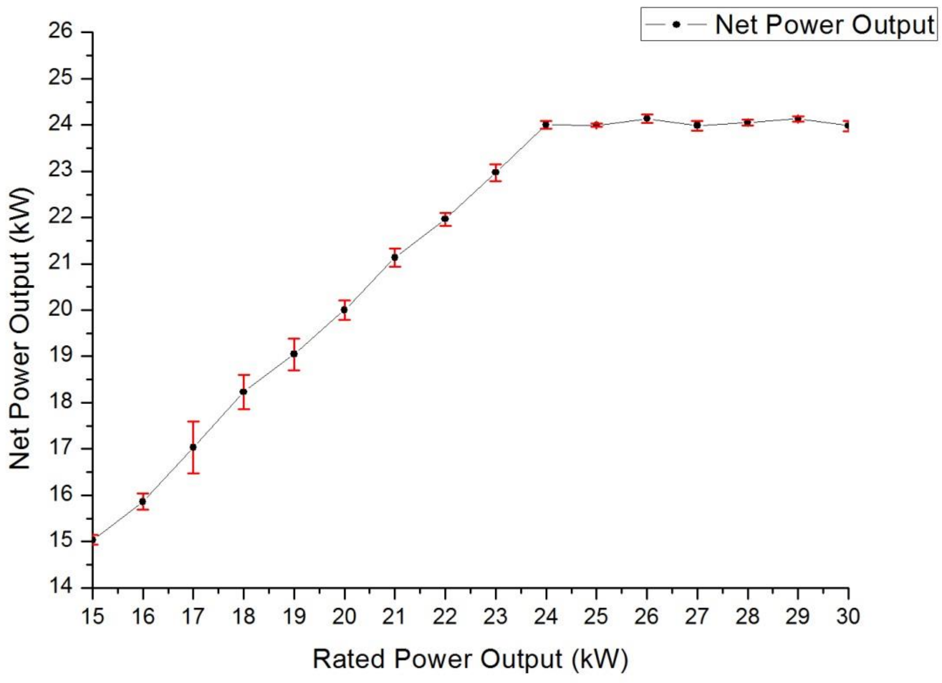

Figure 3.13 Experimental Error Bars for Net Power Output at 31.4 ^{o}C

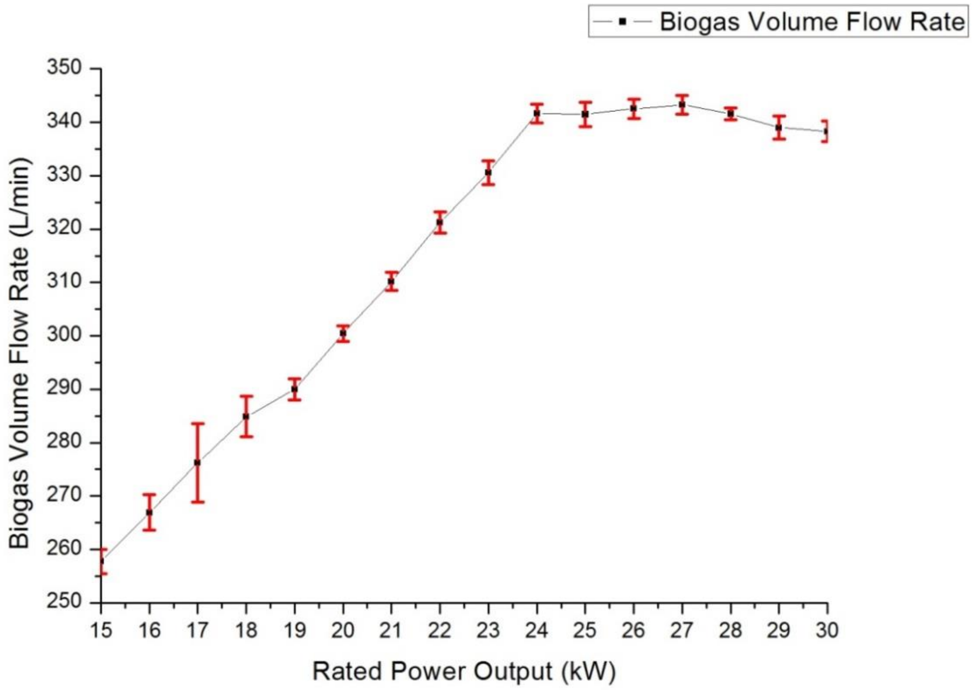

Figure 3.14 Experimental Error Bars for Biogas Volume Flow Rate at 31.4 ^{o}C

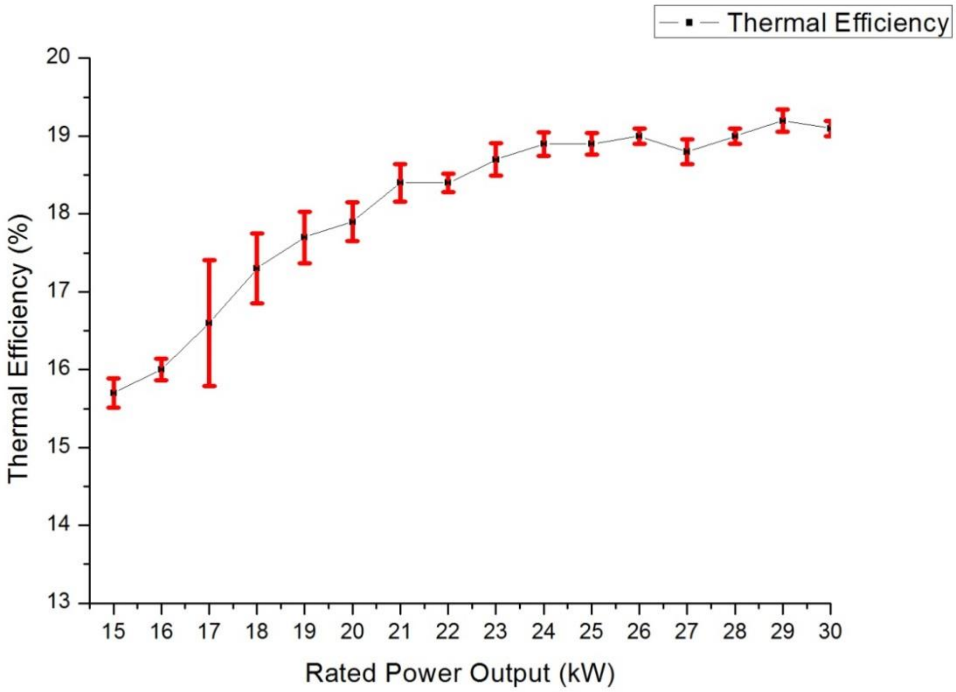

Figure 3.15 Experimental Error Bars for Thermal Efficiency at 31.4 ^{o}C

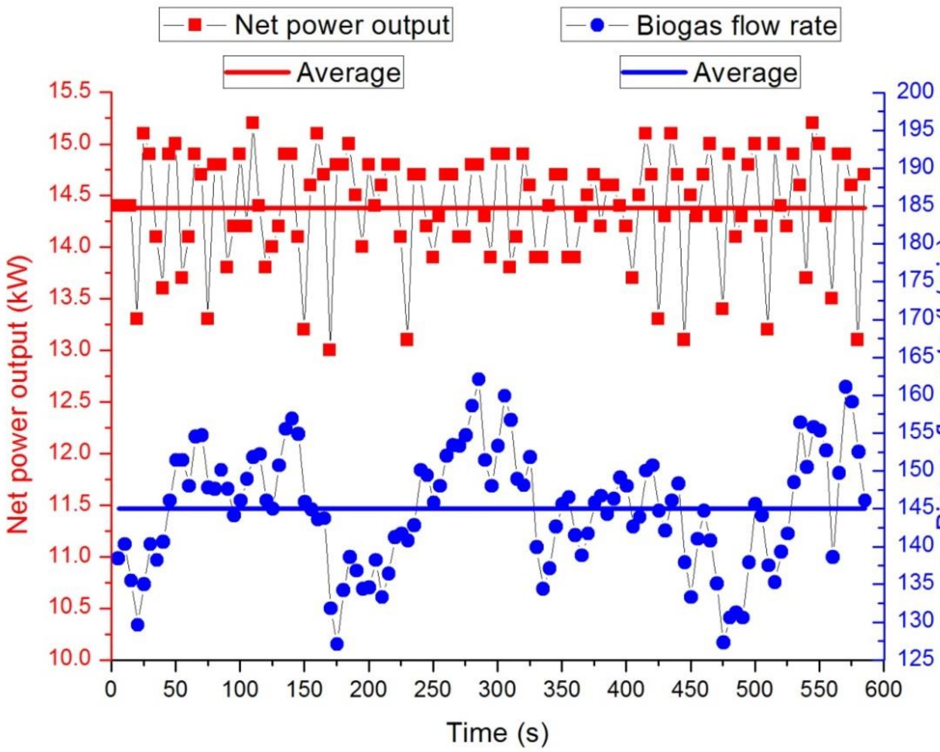

Figure 3.16 CR30 System Stability in 15 kW

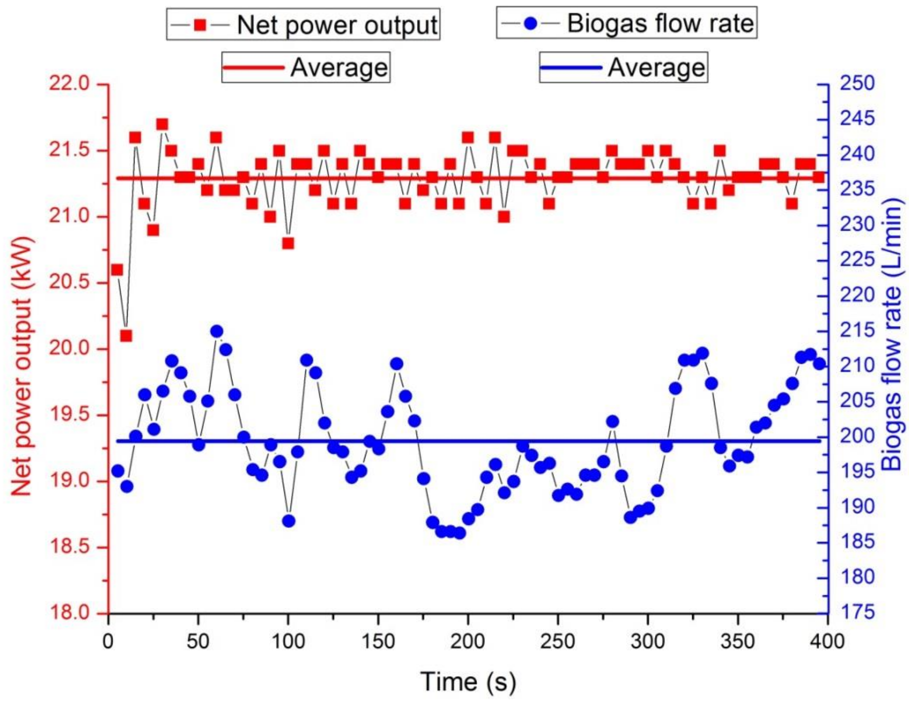

Figure 3.17 CR30 System Stability in 22 kW

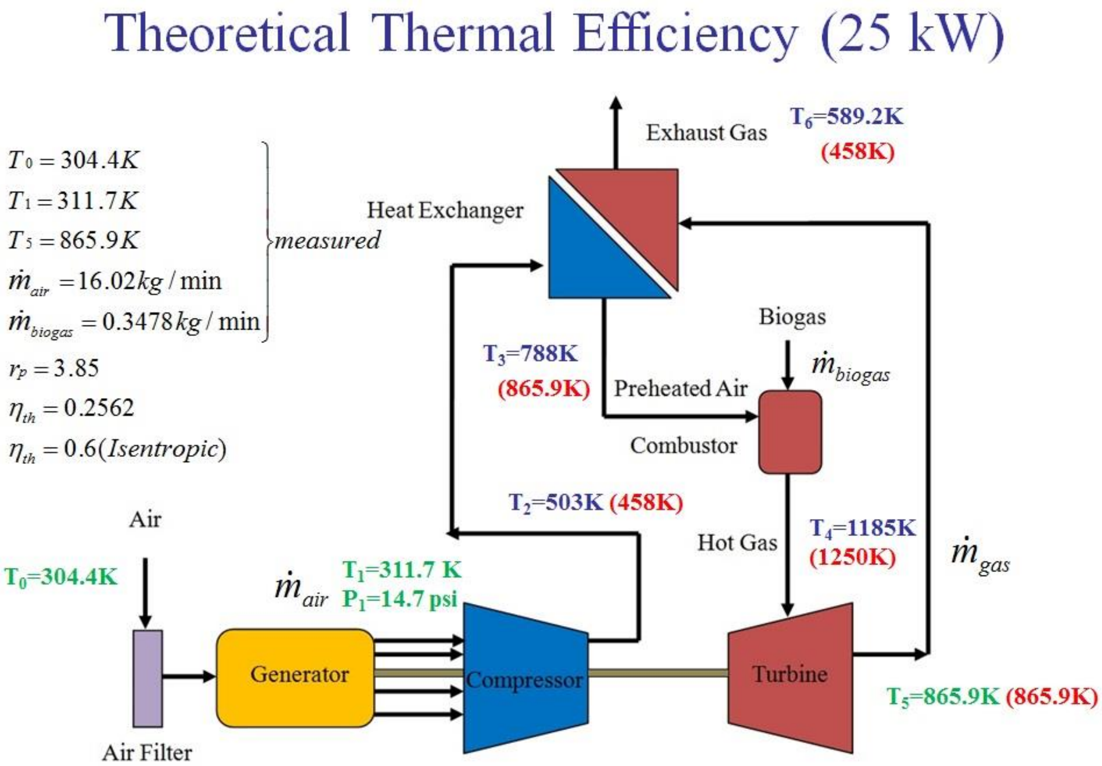

Figure 4.1 The Calculation of the Theoretical Thermal Efficiency in 25 kW at 31.4 ^{o}C

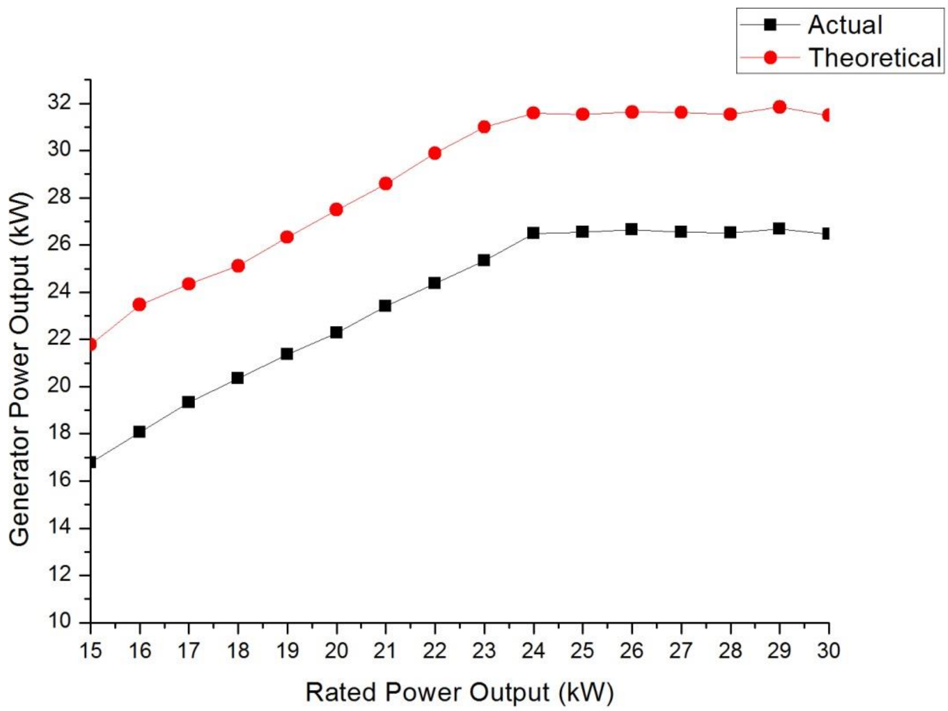

Figure 4.2 Generator Power Output V.S. Rated Power Output

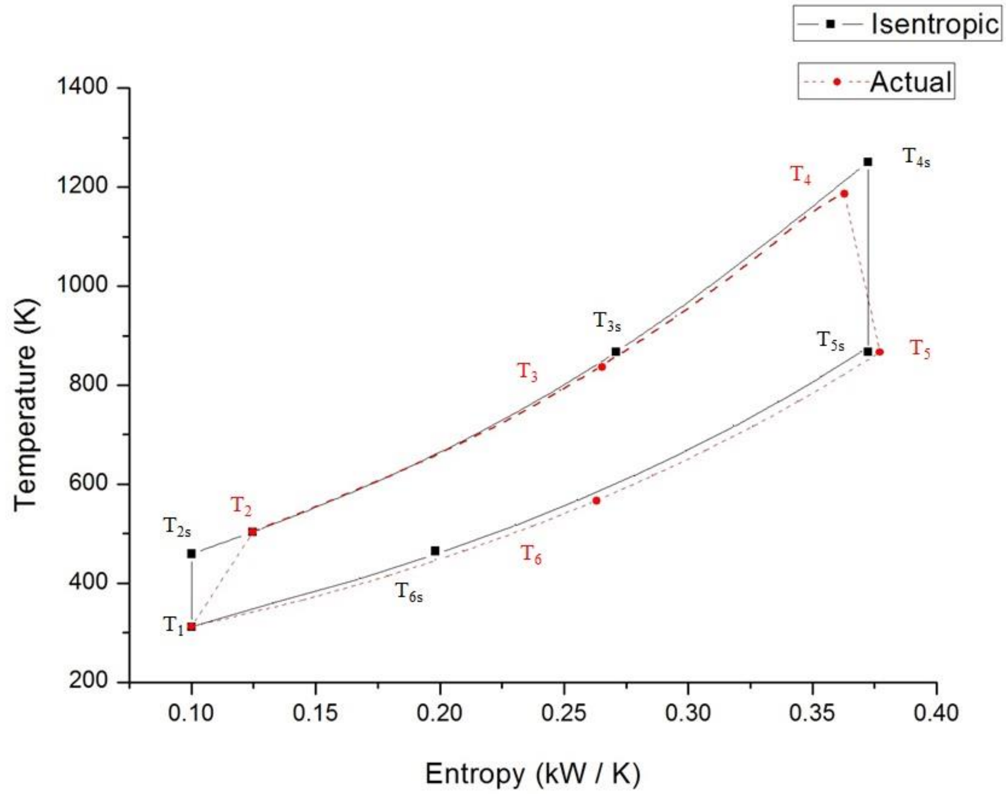

Figure 4.3 T-S Diagram for Gas Turbine Engine at 31.4 °C

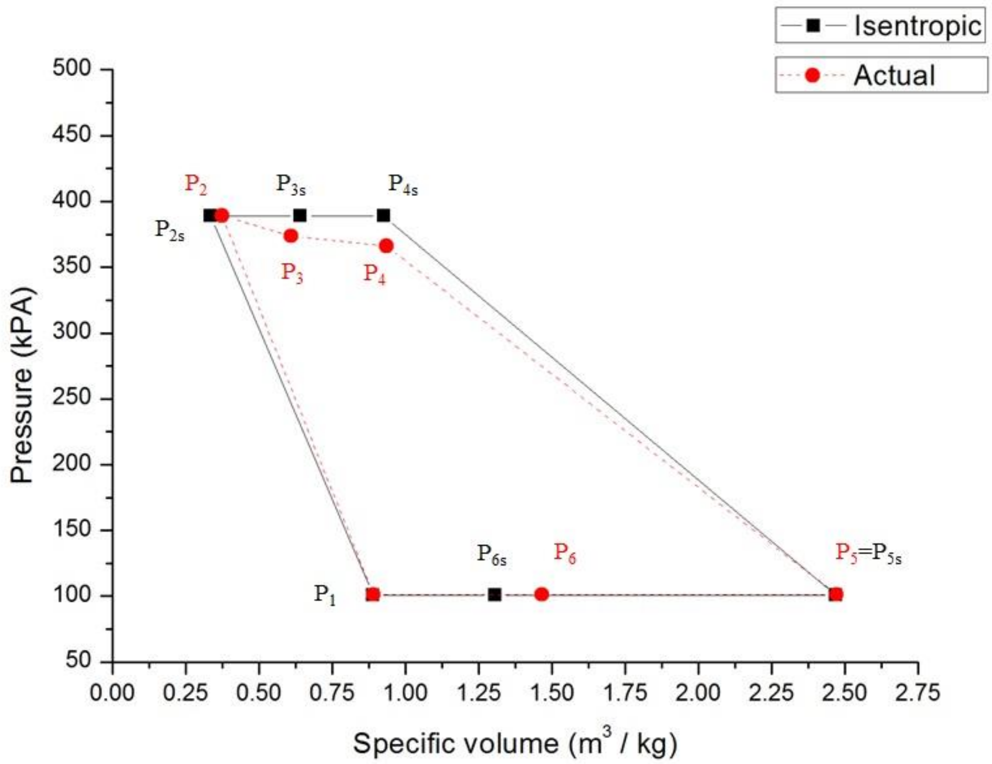

Figure 4.4 P-V Diagram for Gas Turbine Engine at 31.4 °C

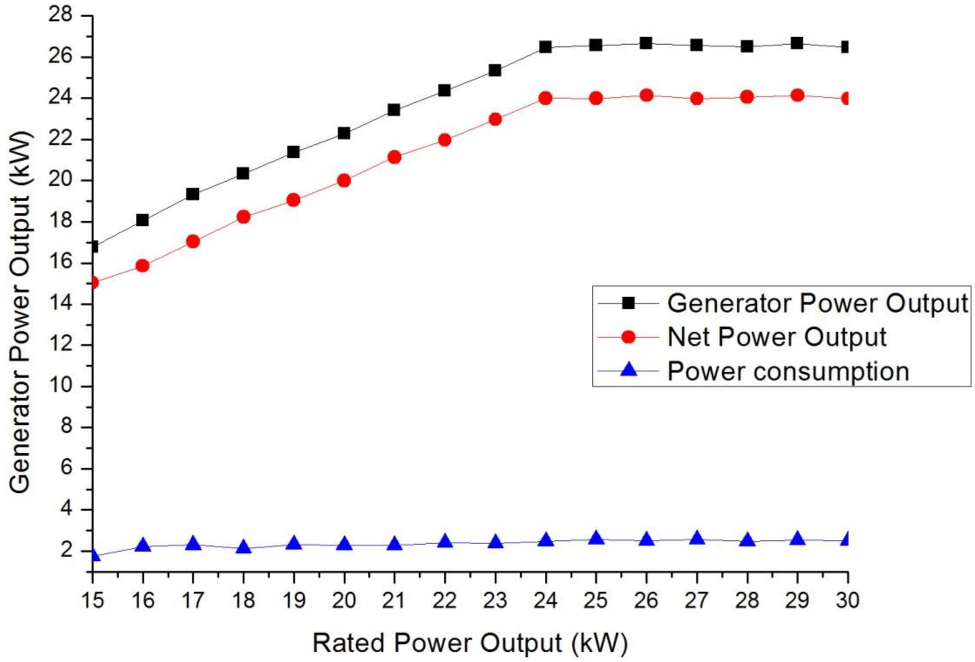

Figure 4.5 Power Consumption of Control System at 31.4 ^{o}C

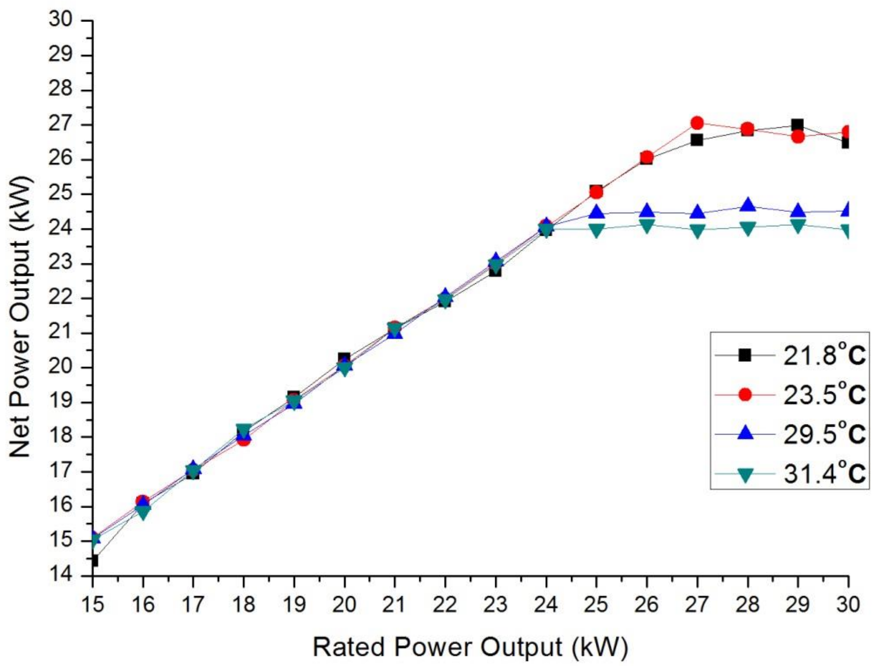

Figure 4.6 Net Power Output v.s. Rated Power Output

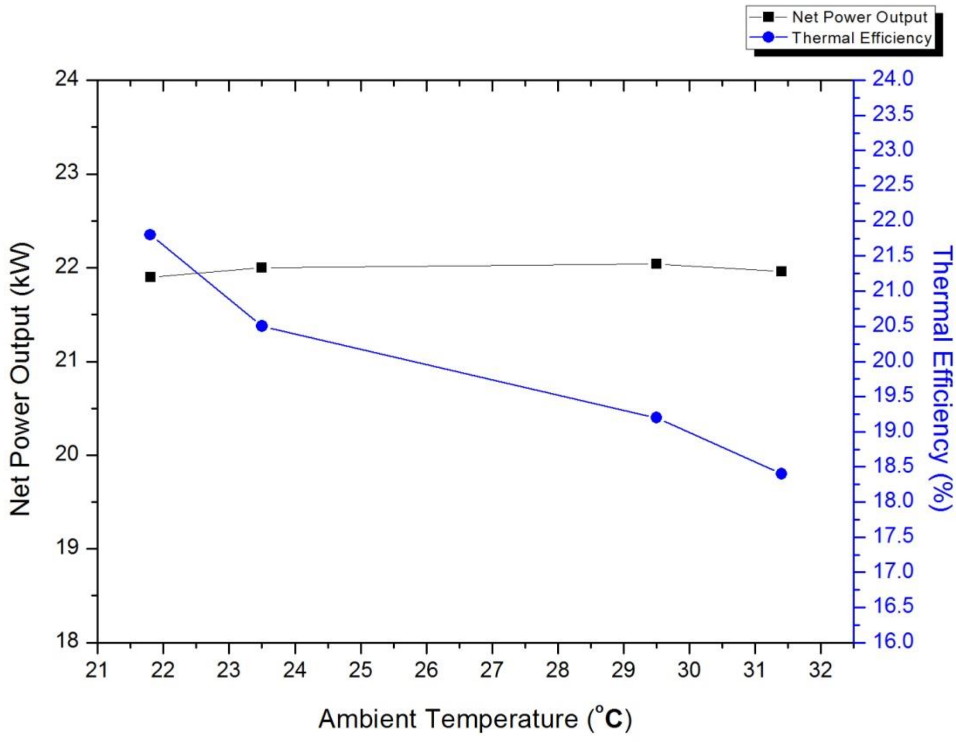

Figure 4.7 Effect of Ambient Temperature in 22 kW

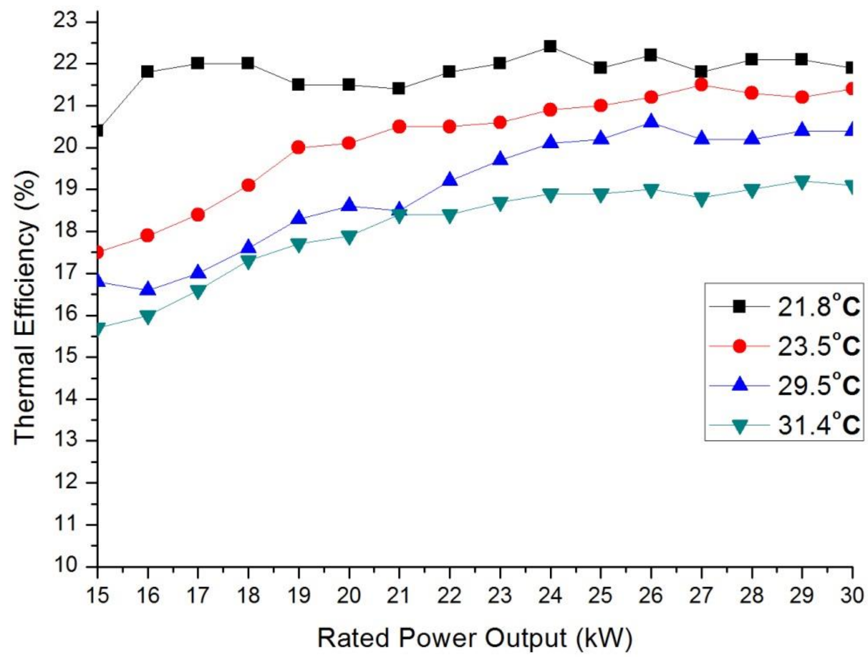

Figure 4.8 Thermal Efficiency v.s. Rated Power Output

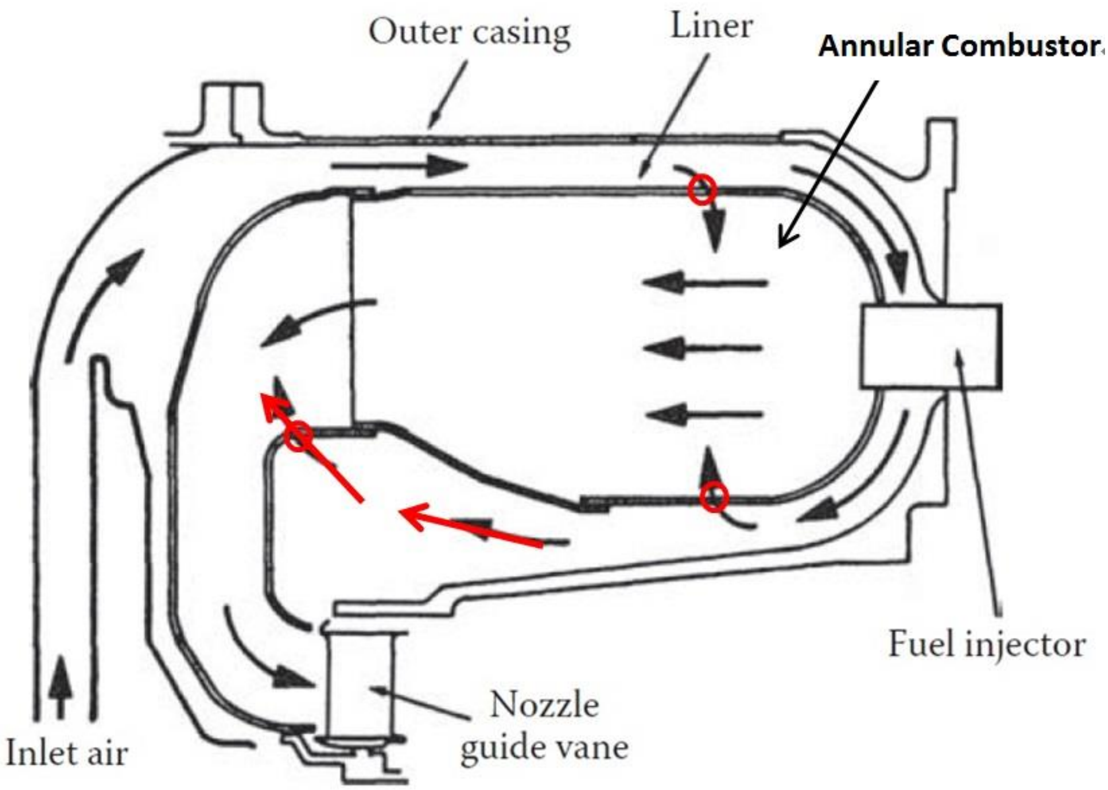

Figure 4.9 Cross-Section of Annular Combustor [27]

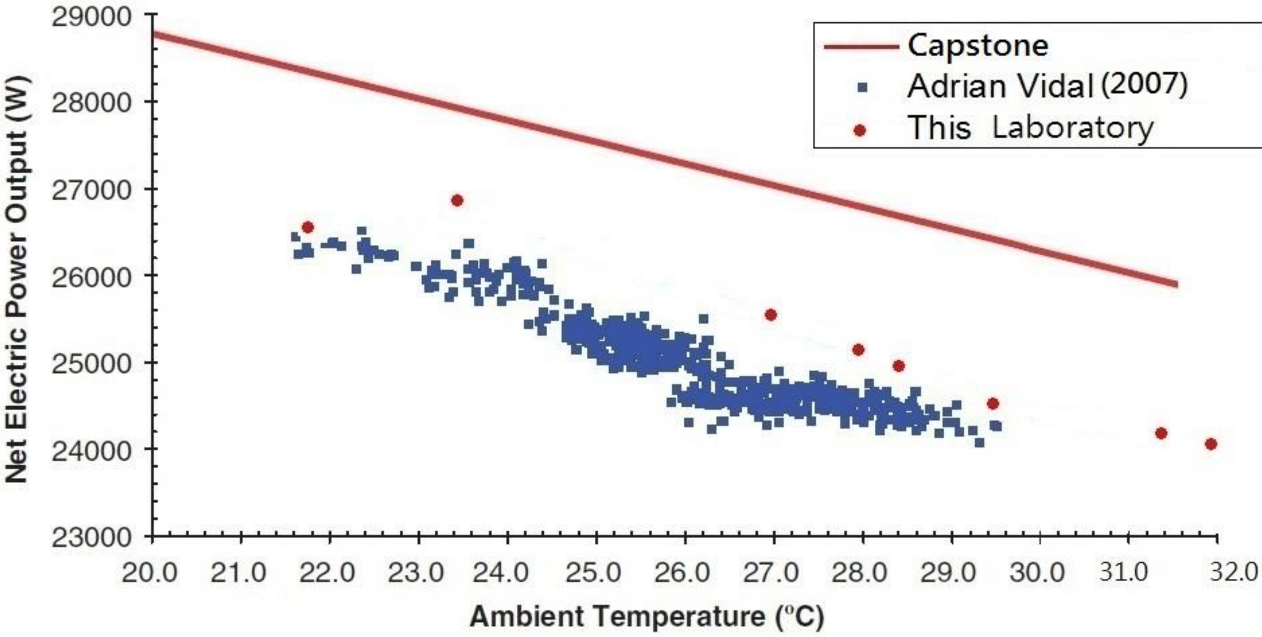

Figure 4.10 Comparison of Net Power Output

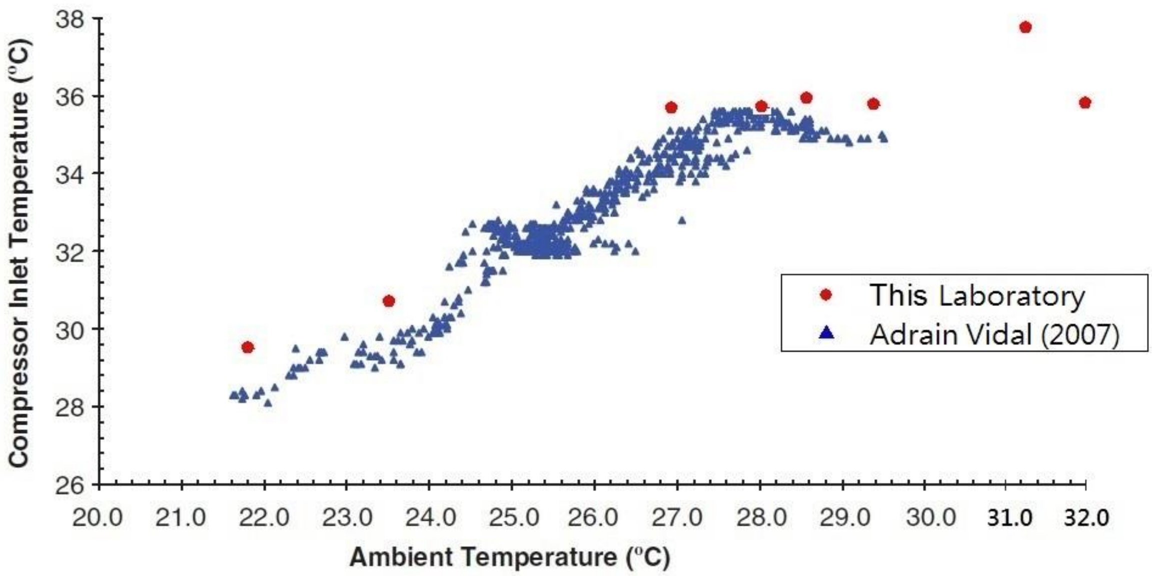

Figure 4.11 Comparison of Compressor Inlet Temperature

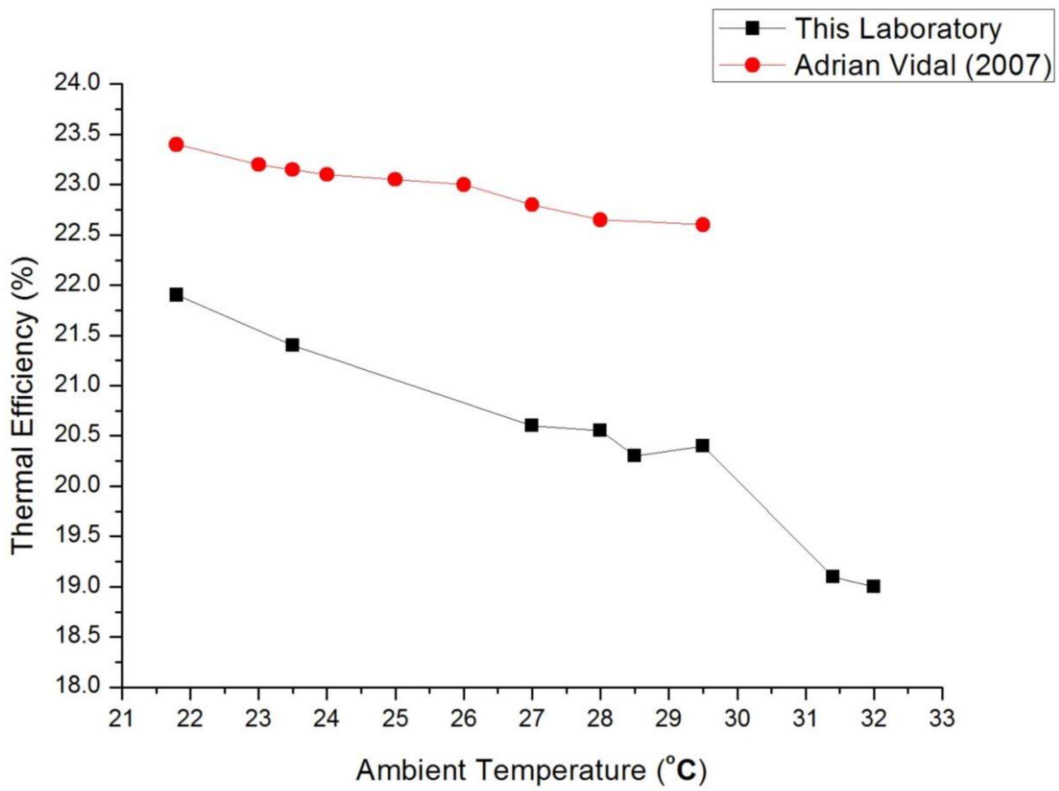

Figure 4.12 Comparison of Thermal Efficiency

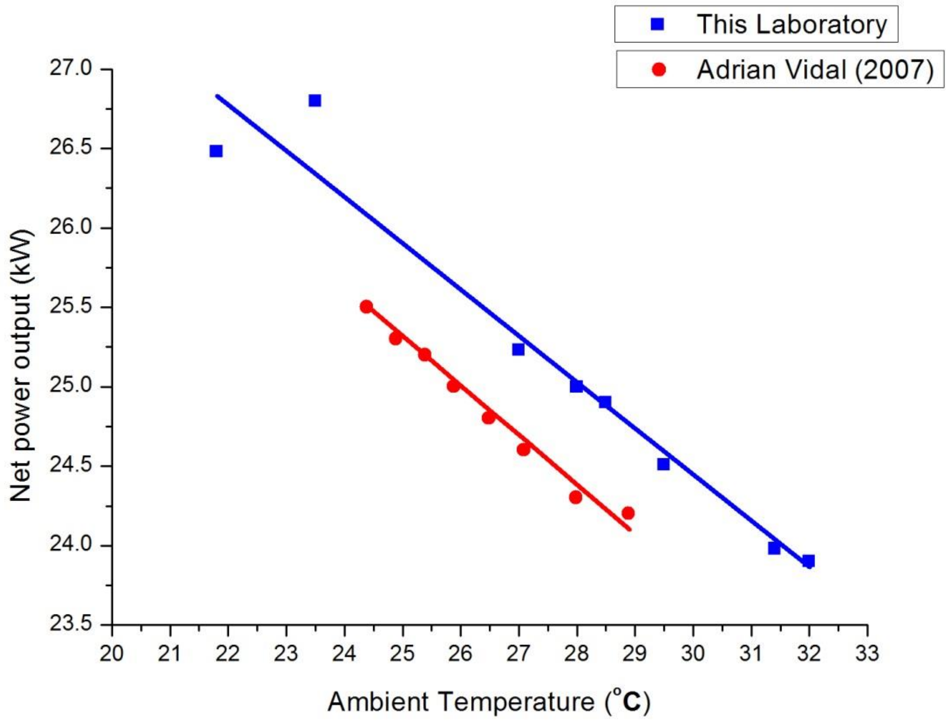

Figure 4.13 Least Square Method for Net Power Output

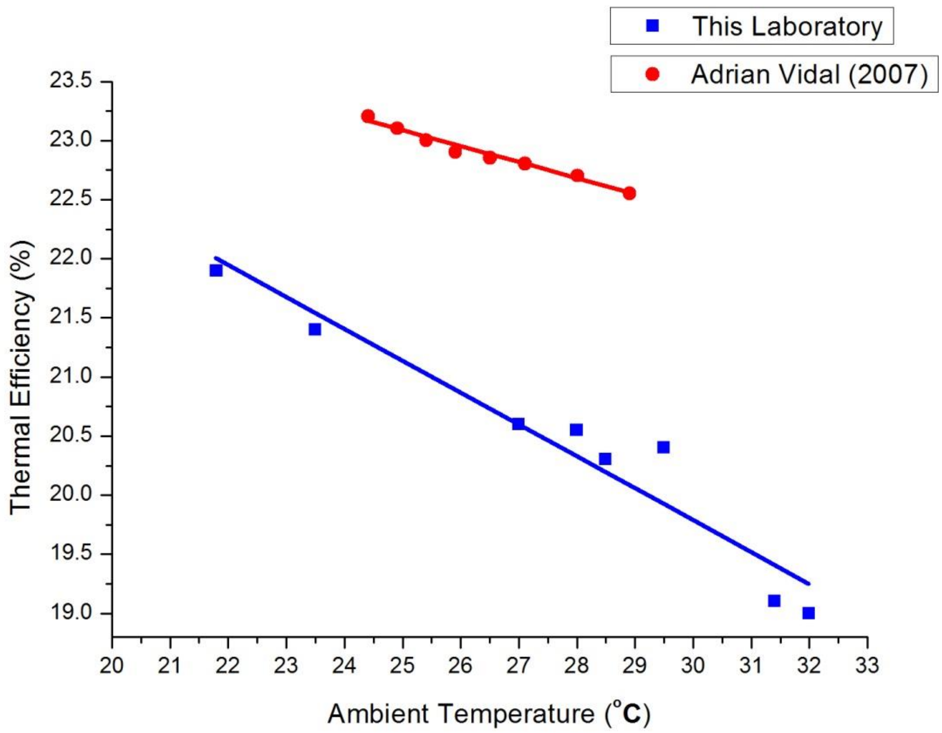

Figure 4.14 Least Square Method for Thermal Efficiency